PIEZOELECTRIC ANALYSIS FOR HETROGENEOUS MEDIUM

by

SOLMAZ TORABI

Presented to the Faculty of the Graduate School of

The University of Texas at Arlington in Partial Fulfillment

of the Requirements

for the Degree of

MASTER OF SCIENCE IN MATERIALS SCIENCE AND ENGINEERING

THE UNIVERSITY OF TEXAS AT ARLINGTON

August 2005

This thesis has been dedicated to my oldest sister,

Dr. Masoumeh Torabi,

who I missed the most

God bless you

ACKNOWLEDGMENTS

I would like to thank Dr. Seiichi Nomura for taking on the role as my advisor. It has been a pleasure and absolute privilege to work under his supervision and I appreciate his advice and patience. Also I would like to thank Dr. Wen Chan and Dr. Pranesh Aswath for taking the time to serve on my committee.

Finally, I would like to thank my loving family and friends. First my parents, Sadegh Torabi and Fariba Mousavi for their love and support while acquiring this degree. I owe all that I have done to some of the great sacrifices they have made to facilitate the course of my life. Next, my sisters, Farkhondeh, Maryam, Leila and Naghmegh and my brother, Majid, for all of their love and support they gave me during my studying at UTA. And last and not least Amin who showed me how great the life can be with a true love, thank you for your patient during writing this thesis.

July 25, 2005

ABSTRACT

PIEZOELECTRIC ANALYSIS FOR
HETROGENEOUS MEDIUM

Publication No. _____

Solmaz Torabi, M.S.

The University of Texas at Arlington, 2005

Supervising Professor: Dr. Seiichi Nomura

In the recent years, several types of piezocomposites have been fabricated since they have provided material properties superior to conventional piezoelectric materials. In order to design these composites, it is essential to find the elastic and electric fields for their different parts, as well as the effective properties of the composite. In the present study, the analytical approach based on the extension of Eshelby's theory in piezoelectricity and the numerical approach based on FEM modeling and ANSYS software have been used to find these elastic and electric fields inside the piezoceramic inhomogeneity for two different piezocomposite according to their connectivity, 0-3 and 1-3. In addition, based on these fields, the effective properties of the piezocomposite have been calculated in the analytical solution and have been compared with the numerical solution results for the effective properties. These comparisons

between two approaches for different volume fractions show the analytical approach is valid to find the inside's fields and the effective properties for less than ten percent of the piezoceramic volume fractions.

TABLE OF CONTENTS

LIST OF ILLUSTRATIONS

LIST OF TABLES

CHAPTER 1

INTRODUCTION

In recent years, several types of piezoceramic composites have been fabricated since piezocomposites provide material properties superior to conventional piezoelectric materials. Piezocomposites have become attractive candidates for use in many applications such as ultrasonic imaging, sensors, actuators, damping, medical imaging and non-destructive evaluation. These materials consist of an active piezoelectric phase and a passive phase, usually a polymer.

Along with the widespread application of piezocomposites, how to determine the effects of defects and inclusions on the properties of such materials becomes one of the most important problems in engineering. For example, a piezocomposite used as a sensor is designed to work under stress and deformation. Thus, various damage and micro-defects in piezocomposite sensor have been observed. Studies on defects (such as dislocations, crack and void) and inhomogeneity inside the piezocomposite material have then attracted the attention of many researchers. For this reason, studying the elastic and electric fields inside and outside piezoceramic part of the piezocomposite is necessary.

In addition to the above reason, in the past few years, much work has been done in the analysis and prediction of the effective properties of piezocomposites according to their importance in the design of these composites. Finding the elastic and electric

fields in different parts of piezocomposite is one way to calculate these effective properties.

The micromechanical characterization and analysis of piezocomposites were launched by Newnham's connectivity theory [1], which is based on the combination of mechanics of materials type parallel and series models. According to his theory, the properties of composites depend on the distribution of the components. The concept of *connectivity* is useful in classifying different types of composites. The basis of this concept is that any phase in a composite may be self-connected in zero, one, two or three dimensions. There are 10 different ways of connecting the phases in a two-phase composite, (0–0, 1–0, 2–0, 3–0, 1–1, 2–1, 3–1, 2–2, 3–2 and 3–3), each described by two numbers, the first defining how the active ceramic phase is connected and the second how the passive polymer phase is connected.

Eshelby's theory [2] is of great importance in various engineering and physical fields, and is the subject of extensive studies. This theorem deals with two related problems in classical elasticity theory. The first one is the determination of the stresses and displacements produced in a medium occupying the entire space if an ellipsoidal subregion undergoes a spontaneous deformation, which would be homogeneous in the absence of the surrounding material. The second one is an analogous problem for the case in which the inclusion and matrix have different elastic constants, while the stresses are induced by a uniform stress-field at infinity.

In approaching above objectives, Eshelby [2] proceeded through a sequence of imaginary cutting, straining, and welding operations, which are claimed to be equivalent

to a formulation of above problems. As a result, elastic field inside the inclusion can be calculated based on Eshelby's theory.

Extension of the well-known Eshelby's inhomogeneity solution from elasticity to the piezoelectric material has been done in details by Wang [3] to find the elastic and electric fields in different parts of piezocomposite.

Wang [3] studied a problem of piezoelectric inclusions in an infinite piezoelectric medium via the Green's function technique to find the integral expressions for the strain and electric fields, but the integral expressions are very complicated, thus closed-form solutions of strain and electric fields are too difficult to obtain even though the matrix is chosen to be non-piezoelectric. Moreover, Wang did not consider the interaction among inclusions.

From the view of stated applications, piezocomposites are made up of a piezoelectric phase and the non-piezoelectric matrix. For example, sensors made of piezoelectric materials, which are widely used in smart materials or smart structures are generally piezoelectric inhomogeneities embedded in a non-piezoelectric matrix in which the elastic fields and the electric fields are decoupled in it.

No electro-mechanical interaction in the matrix material assumption, a non-piezoelectric medium, has been used in many studies to obtain the coupled elastic and electric fields inside the piezoelectric inhomogeneity in the matrix. Fan and Qin [4] analyzed a piezoelectric ellipsoidal inhomogeneity embedded in a non-piezoelectric elastic matrix via the equivalent inclusion method of Eshelby's theory. They used a simple way to find the elastic and electric fields inside the inhomogeneity. They applied

non-piezoelectric elastic matrix assumption to partially decouple the original piezoelectric inhomogeneity problem, although the coupling still holds inside the inhomogeneity.

Based on Fan and Qin's analytical approach and the finite element approach, the elastic and electric fields inside the piezoelectric spherical and ellipsoidal inhomogeneities embedded in a non-piezoelectric elastic matrix have been analyzed in the present thesis. Also the effective coefficients have been calculated through these two ways, an analytical and a numerical approach.

To do all the above calculation, it is necessary to know the piezoelectric characters and formulations, which are given in Chapter 2. The analytical solution is based on the analysis of the coupled elastic field and electric field of a typical piezoelectric inhomogeneity in a non-piezoelectric medium. To do this analysis, it is essential to know the original Eshelby's theory for the elastic problems and extension of Eshelby's theory to piezocomposites, which are given in Chapter 3 and 4, respectively. For the numeric approach ANSYS, commercial finite element software, has been used. For this approach, Chapter 5 has been provided to teach some basic steps in using this software in piezoelectric modeling. The result of these two ways is given and compared in Chapter 6 and the conclusion of this study has been provided in Chapter 7.

CHAPTER 2

PIEZOELECTRIC CERAMICS

2.1 Background Theory

All materials undergo a small change in dimensions when subjected to an electric field. If the resultant strain is proportional to the square of the field, it is known as the electrostrictive effect. Some materials show the reverse effect – the development of electric polarization when they are strained through an applied stress. This is called the direct piezoelectric effect. Piezoelectricity is a property possessed by a group of materials, discovered in 1880 by Pierre and Jacques Curie, during their study of the effects of pressure on the generation of electrical charge by crystals such as Quartz, tourmaline and Rochelle salt. Piezoelectricity stems from the Greek word *piezo* for pressure.

Piezoelectricity is a linear effect that is related to the microscopic structure of the solid. Some ceramic materials become electrically polarized when they are strained; this linear and reversible phenomenon is referred to as *the direct piezoelectric effect*; and it is always accompanied by *the converse piezoelectric effect* where a solid becomes strained when placed in the electric field. The microscopic origin of the piezoelectric effect is the displacement of ionic charged within a crystal structure. In the absence of external strain, the charge distribution within the crystal is symmetric and the net

electric dipole moment is zero. However, when an external stress is applied, the charges are displaced and the charge distribution is no longer symmetric. A net polarization develops and results in an internal electric field. A material can only be piezoelectric if the unit cell has no center of inversion. The lack of center of symmetry means that a net movement of the positive and negative ions with respect to each other, as a result of stress, produces an electric dipole. The ceramic, being composed of the random orientation of these piezoelectric crystallites, is inactive, i.e., the effects from the individual crystals cancel each other and no discernable piezoelectricity is present. Regions of equally oriented polarization vectors are known as domains. [5]

Among the 32 classes of single-crystal materials, 11 possess a center of symmetry and are non-polar. For these, an applied stress results in symmetrical ionic displacements so that there is no net change in dipole moment. The other 21 crystal classes are non-centrosymmetric, and 20 of these exhibit the piezoelectric effect. The single exception, in the cubic system, possesses symmetry characteristics, which combine to give no piezoelectric effect. [6]

Piezoelectric materials commercialize with the discovery of barium titanate and zirconate titanate (*PZT*) in the 1940s and the 1950s, respectively. These family of materials exhibited very high dielectric and piezoelectric properties. Furthermore, their behavior to specific responses and applications can be modified by the use of dopants. Today, *PZT* is one of the most widely used piezoelectric materials. It is noted that most commercially available ceramics, such as barium titanate and *PZT*, are based on the perovskite structure, Fig 2.1.

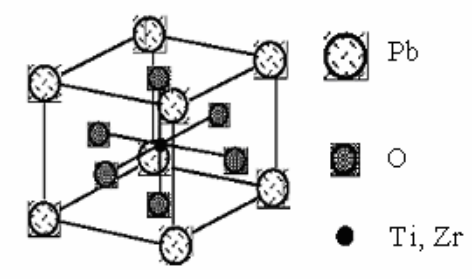

Fig. 2.1 Pervoskite structure [5]

The fabrication of most bulk piezoelectric ceramics is the same as other ceramics except that they have one more process called *poling*. *Poling* is a commonly used method to orient the domains by polarizing the ceramic through the application of a static electric field. The electrodes are applied to the ceramic and a sufficiently high electric field, a strong DC filed, is applied such that the domains rotate and switch in the direction of the electric field in the polycrystalline ceramic. The result is never a full orientation of all domains; however, the polycrystalline ceramic exhibits a large piezoelectric effect. During this process, there is a small expansion of the material along the poling axis and a contraction in both directions perpendicular to it, see Fig 2.2 [5].

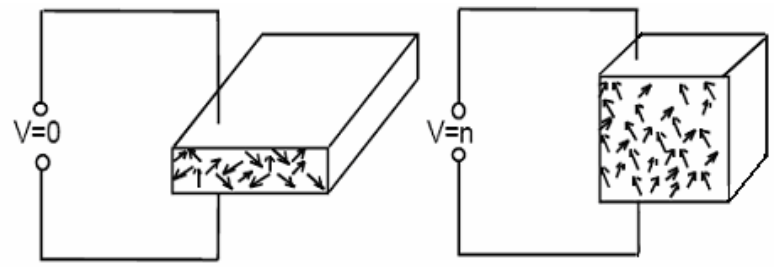

Fig. 2.2 Polling of a piezoelectric ceramic [5]

Polycrystalline materials in which the crystal axes of the grains are randomly oriented all behave electrostrictively whatever the structural class of the crystallites comprising them. If the crystals belong to a piezoelectric class and their crystal axes can be suitably aligned, then a piezoelectric polycrystalline ceramic becomes possible.

It should be noted that a poling process is often necessary with single-crystal ferroelectric bodies because they contain a multiplicity of randomly oriented domains. There is, therefore, a sequence of states of increasing orderliness: polycrystalline ferroelectric ceramics, poled ferroelectric ceramics, single-crystal ferroelectrics and single-domain single crystals.

If a piezoelectric plate, as shown in Fig. 2.3, polarized in the direction indicated by P, carries electrodes over its two flat faces, then a compressive stress causes a transient current to flow in the external circuit; a tensile stress produces a current in the opposite sense, see Fig. 2.3(a). Conversely, the application of an electric field produces strain in the crystal, a negative strain; reversal of the field causes a positive strain, see Fig. 2.3(b). The changes in polarization which accompany the direct piezoelectric effect manifest themselves in the appearance of charges on the crystal surface and, in the case of a closed circuit, in a current.

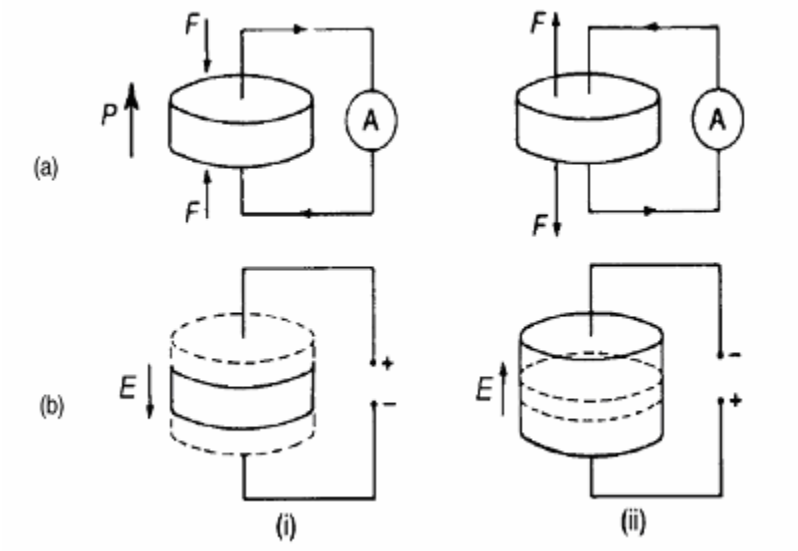

Fig. 2.3 (a) The direct and (b) the indirect piezoelectric effects: (i) contraction; (ii) expansion (The broken lines indicate the original dimensions) [6]

2.2 Piezoelectric Ceramics Coefficients and Equations

Piezoelectric properties are described in terms of the parameters D, E, σ and ε; where D is the electrical displacement, also referred to in ANSYS as the electric flux density, E is the electric field, σ is the mechanical stress and ε is the mechanical strain. The electrical response according to the direct effect can be expressed in terms of strain by

$$D = e\,\varepsilon, \tag{2.1}$$

where e is piezoelectric constants and relating the stress and the electric field and the converse effect can be expressed by

$$\sigma = e\,E. \tag{2.2}$$

The equations of piezoelectric state in all terms can be written as

$$\sigma = C^{E}\,\varepsilon - e\,E, \tag{2.3}$$

$$D = e\,\varepsilon + K^{\varepsilon}\,E, \tag{2.4}$$

where C^E is the elastic stiffness at a constant electric field, i.e. short circuit, and K^{ε} is the permittivity or dielectric constant at constant strain, i.e. mechanically clamped.

Most of the literatures use the above relationship in the following form:

$$\varepsilon = s^E\,\sigma + d\,E, \tag{2.5}$$

$$D = d\,\sigma + K^{\sigma}\,E, \tag{2.6}$$

where s^E is the elastic compliance evaluated at constant electric field, i.e. short circuit, d is the piezoelectric tensor relating the strain and the electric field, K^{σ} is the permittivity at constant stress, i.e. mechanically free. As stated in the first Chapter, two approaches, numerical and analytical will be studied in this thesis. For the numerical method ANSYS software has been used, and this software requires equations in the format of equations (2.3) and (2.4). Therefore this format will be used in this Chapter. See Chapter 5 for converting of equation (2.5) and (2.6) to (2.3) and (2.4), respectively.

Another important parameter in piezoceramics is the electromechanical coupling coefficient, k, measuring the ability of a piezoelectric material in transforming mechanical energy into electrical energy, and vice versa. Piezoceramic with higher electromechanical coupling coefficient has more applications. In practice, the energy transfer electrical to mechanical (or vice versa) occurs in a complex 3-dimensional way. The strains caused by applied electrical or mechanical stresses have components in three orthogonal directions necessitating the description of the piezoelectric effect in terms of tensors, as outlined in the next paragraph.

The state of strain in a body is fully described by a second-rank tensor, a *strain tensor*, and the state of stress by a *stress tensor*, again of second rank. Therefore, the relationship between the stress and strain tensors is *fourth-rank tensor*. The relationship between the electric field and electric displacement, i.e. the permittivity, is a *second-rank tensor*. So one can rewrite equation (2.3) and (2.4) in the tensorial format as

$$\sigma_{ij} = C^{E}_{ijkl}\, \varepsilon_{kl} - e_{kij} E_{k,}, \tag{2.7}$$

$$D_i = e_{ikl}\, \varepsilon_{kl} + K^{\varepsilon}_{ik}\, E_k. \tag{2.8}$$

Note that in tensorial notation, if an index occurs twice in any one term, summation is taken from 1 to 3.

In general, a vector, formally regarded as a first-rank tensor, has three components, a second-rank tensor has nine components, a third-rank tensor has 27 components and a fourth-rank tensor has 81 components.

Not all the tensor components are independent. Between equations (2.7) and (2.8) there are 45 independent tensor components, 21 for the elastic modulus C^E, 6 for the permittivity and 18 for the piezoelectric coefficient, e. Fortunately crystal symmetry and the choice of reference axes reduce the number even further.

So far all the equations have been developed in full tensor notation. But when calculating actual properties, it is advantageous to reduce the number of suffixes as much as possible. This has been done by defining new symbols. As a result, the tensor will be reduced to matrix notation. So instead of the above tensor notation, matrix notation can be employed to represent equations (2.7) and (2.8) as

$$\begin{pmatrix}\sigma\\ D\end{pmatrix}=\begin{pmatrix}C^E-e\\ e^T\ \ K^\varepsilon\end{pmatrix}\begin{pmatrix}\varepsilon\\ E\end{pmatrix}, \tag{2.9}$$

where the superscript T denotes the transpose of a matrix. The stress and strain tensors can be represented by the vectors of their components as

$$[\sigma]=\begin{pmatrix}\sigma_{11}\\ \sigma_{22}\\ \sigma_{33}\\ \tau_{23}\\ \tau_{13}\\ \tau_{12}\end{pmatrix} \text{ and } [\varepsilon]=\begin{pmatrix}\varepsilon_{11}\\ \varepsilon_{22}\\ \varepsilon_{33}\\ \gamma_{23}\\ \gamma_{13}\\ \gamma_{12}\end{pmatrix}. \tag{2.10 and 11}$$

The vector of E and tensors of D and K^ε remain unchanged with respect to equations (2.7) and (2.8) as

$$[E]=\begin{pmatrix}E_1\\ E_2\\ E_3\end{pmatrix},\ [D]=\begin{pmatrix}D_1\\ D_2\\ D_3\end{pmatrix} \text{ and } [K]^\varepsilon=\begin{pmatrix}K_{11} & K_{12} & K_{13}\\ K_{21} & K_{22} & K_{23}\\ K_{31} & K_{32} & K_{33}\end{pmatrix}^\varepsilon. \tag{2.12, 13 and 14}$$

By defining new symbols, the relation between tensors C^E_{ijkl} and e_{ijk} as stated in the equation (2.7) and components of matrix C^E and e, C^E_{pq} and e_{ip} (where $i = 1\rightarrow 3$, p and $q = 1\rightarrow 6$) will be determined by the following rule

ij or kl	11	22	33	32 or 23	31 or 13	12 or 21
p or q	1	2	3	4	5	6.

(2.15)

For instance, $C_{11}= C_{1111}$, $C_{14}=\frac{1}{2}\ C_{1132}$, $C_{55}=\frac{1}{4}\ C3131$, $e_{14}=\frac{1}{2}\ e_{123}$ and so on. Note with considering the multiple appearances of some elements in the original equations (2.7)

and (2.8), there is no need to put these fractions. According to the above rule, the matrix of piezoelectricity can be written as

$$[e]^T = \begin{pmatrix} e_{11} & e_{12} & e_{13} & e_{14} & e_{15} & e_{16} \\ e_{21} & e_{22} & e_{23} & e_{24} & e_{25} & e_{26} \\ e_{31} & e_{32} & e_{33} & e_{34} & e_{35} & e_{36} \end{pmatrix}, \tag{2.16}$$

and the stiffness matrix will be

$$[C]^E = \begin{pmatrix} C_{11} & C_{12} & C_{13} & C_{14} & C_{15} & C_{16} \\ C_{21} & C_{22} & C_{23} & C_{24} & C_{25} & C_{26} \\ C_{31} & C_{32} & C_{33} & C_{34} & C_{35} & C_{36} \\ C_{41} & C_{42} & C_{43} & C_{44} & C_{45} & C_{46} \\ C_{51} & C_{52} & C_{53} & C_{54} & C_{55} & C_{56} \\ C_{61} & C_{62} & C_{63} & C_{64} & C_{65} & C_{66} \end{pmatrix}. \tag{2.17}$$

The convention is to define the poling direction as the 3-axis, as illustrated in Fig. 2.4. The shear planes are indicated by the subscripts 4, 5 and 6 and are perpendicular to directions 1, 2 and 3, respectively. For example, e_{31} is the coefficient relating the field along the polar axis to the stress, or strain, perpendicular to it, while e_{33} is the corresponding coefficient for either stress, or strain, and field along the polar axis. Shear can only occur when a field is applied at right angles to the polar axis so that there is only one coefficient, e_{15}.

According to *Neumann's* principle, the symmetry element of any physical property of a crystal must include the symmetry elements of the point group of the crystal. Application of this principle can reduce the number of independent components.

Here the discussion is restricted to poled polycrystalline ceramics, which have

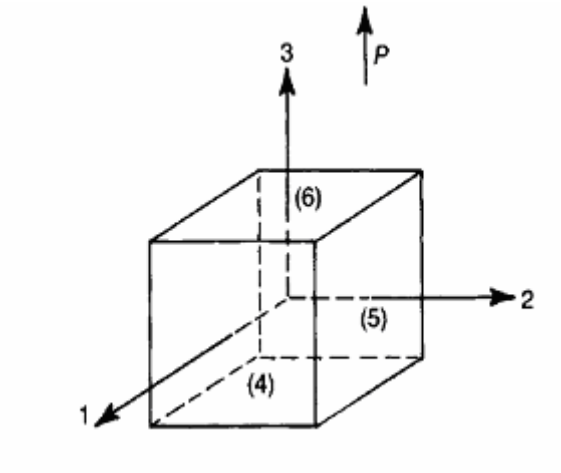

Fig. 2.4 Labeling of reference axes and planes for piezoceramics [6]

initially isotropic. In poling direction, this isotropy is destroyed. In the direction perpendicular to the poling direction, material is transversely isotropic. The symmetry elements are an axis of rotation of infinite order in the direction of poling and an infinite set of planes parallel to the polar axis as reflection planes. The symmetry of a poled ceramic is therefore described as ∞mm, which is equivalent to *6mm* in the hexagonal symmetry system. According to this symmetry, 5 components for the elastic stiffness C^E, 2 for the permittivity and 3 for the piezoelectric coefficient, e, will be independent; note the multiple appearance of some elements [5, 6]. With this symmetry of transversely isotropic piezoceramic material and considering poling direction at 3, $[C]^E$, $[e]^T$, and $[K]^\varepsilon$ will reduce to

$$[K]^\varepsilon = \begin{pmatrix} K_{11} & 0 & 0 \\ 0 & K_{11} & 0 \\ 0 & 0 & K_{33} \end{pmatrix}^\varepsilon, \tag{2.18}$$

$$[e]^T = \begin{pmatrix} 0 & 0 & 0 & 0 & e_{15} & 0 \\ 0 & 0 & 0 & e_{15} & 0 & 0 \\ e_{31} & e_{31} & e_{33} & 0 & 0 & 0 \end{pmatrix}, \tag{2.19}$$

$$[C]^E = \begin{pmatrix} C_{11} & C_{12} & C_{13} & 0 & 0 & 0 \\ C_{12} & C_{11} & C_{13} & 0 & 0 & 0 \\ C_{13} & C_{13} & C_{33} & 0 & 0 & 0 \\ 0 & 0 & 0 & C_{44} & 0 & 0 \\ 0 & 0 & 0 & 0 & C_{44} & 0 \\ 0 & 0 & 0 & 0 & 0 & \frac{C_{11} - C_{12}}{2} \end{pmatrix}. \tag{2.20}$$

2.3 Piezoelectric Composites

The reciprocity in energy conversion makes piezoelectric ceramics such as *PZT* very attractive materials especially towards sensors and actuators applications. Even if their properties make them interesting, they are often limited, first by their weight, that can be a clear disadvantage for shape control and as a consequence, by their high specific acoustic impedance, which reduces their acoustic matching with the external fluid domain. Bulk piezoelectric materials have several drawbacks; hence composite piezoelectric materials are often a better technological solution in the case of a lot of applications such as ultrasonic transducers, medical imaging, sensors, actuators and damping. Composite technology in general sets out to combine materials in such a way that the properties of the composite are the optimum for a particular application. The property, whether mechanical, thermal, or electrical, is determined by the choice of component and their relative amounts and, most importantly, the connectivity, that is the manner in which the components are interconnected [7].

Piezoceramic-polymer composites are a relatively recent addition to the range of composite materials and have been developed principally because their properties offer advantages, especially for sonar and medical ultrasonic imaging technologies, over those of the piezoceramics alone. For these applications, the transducer is usually interfacing with water or soft tissue, for example body skin. The advantages include relatively good acoustic matching between the transducer and the medium, improved electromechanical coupling coefficients and well-defined ultrasonic pulses. [6]

The properties of composites depend on the distribution of the components. The concept of *connectivity* is useful in classifying different types of composites. The basis of this concept is that any phase in a composite may be self-connected in zero, one, two or three dimensions. There are 10 different ways of connecting the phases in a two-phase composite, (0–0 to 3–3), each described by two numbers, the first defining how the active ceramic phase is connected and the second how the passive polymer phase is connected [1]. In this study attention is confined to the two most commonly encountered connectivities, 0–3 and 1–3.

The 0-3 composite is a mixture of randomly dispersed and separated particles having a connectivity of zero, because the ceramic phase is not continuous in any direction, while the matrix surrounding them having a connectivity of three, because it is continuous in all three orthogonal directions. A 1–3 composite consists of piezoceramic rods extending from electrode to electrode and embedded in a polymer. The rods have one-dimensional connectivity and the polymer again three-dimensional connectivity.

CHAPTER 3

ESHELBY'S THEORY FOR PURE ELASTIC PROBLEM

3.1 Background Theory

In the physics of solids, a number of problems present themselves in which the uniformity of an elastic medium is disturbed by a region within it which has changed its form or which has elastic constants differing from those of the remainder. Some of these problems may be solved for a region of arbitrary shape. Others are intractable unless the region is some form of an ellipsoid. Fortunately, the general ellipsoid is versatile enough to cover a wide variety of particular cases.

When a twin forms inside a crystal, the material is left in a state of internal stress since the natural change of shape of the twinned region is restrained by its surroundings. A similar state of strain arises if a region within the crystal alters its unconstrained form because of thermal expansion, martensitic transformation, precipitation of new phase with different unit cell, or for some other reason. These examples suggest the following general problem in the theory of elasticity [2].

3.1.1 The Transformation Problem

A region, the inclusion, in an infinite homogeneous elastic medium undergoes a change of shape and size which, but for the constraint imposed by its surroundings, the matrix, would be an arbitrary homogeneous strain. What is the elastic strain of inclusion

and matrix? There are different methods to find this elastic field. One of the most famous one is referred as Eshelby's Theory.

According to this theory, one can solve this problem with the help of a simple set of imaginary cutting, straining and welding operations. Cut round the region, which is to transform and remove it from the matrix. Allow the unconstrained transformation to take place. Apply surface tractions chosen so as the restore the region to its original form; put it back in the hole in the matrix and rejoin the material across the cut. The stress is now zero in the matrix and has a known constant value in the inclusion. The applied surface traction has become built in as a layer of body force spread over the interface between the matrix and the inclusion. To complete the solution, this unwanted layer is removed by applying an equal and opposite layer of body force; the additional elastic filed thus introduced is found by integration from the expression for the elastic field of a point force [2].

So far nothing has been assumed about the shape of inclusion. However, Eshelby has showed that if it is an ellipsoid, the stress within the inclusion is uniform. By considering this fact, one can use the solution of the transformation problem as a convenient way in solving a second set of elastic problems. Superimpose on the whole solid a uniform stress, which just annuls the stress in the inclusion. The removal of unstressed inclusion to leave a hole with stress-free surface is then a mere formality, and we have solved the problem of perturbation of a uniform stress field by an ellipsoid cavity. More generally, suppose that the uniformly applied stress does not annul the stress in the inclusion. Then the stress and strain in the inclusion are not related by the

Hooke's law of the material since part of the strain arises from a non-elastic twinning or other transformation with which no stress is associated. The stress and strain are, however, related by Hooke's law of some hypothetical material and transformed the ellipsoid may be replaced by an ellipsoid of the hypothetical material which has suffered the same total strain, but purely elastically. So the following problem has been solved.

3.2 General Theory of Eigenstrains

Eigenstrain is a generic name given to such nonelastic strains as thermal expansion, phase transformation, initial strains, plastic strains and misfit strains. *Eigenstress* is a generic name given to self-equilibrated internal stresses caused by one or several of these eigenstrains in bodies which are free from any other external forces and surface constraints. The eigenstress fields are created by the incompatibility of the eigenstrains [8].

The actual strain is then the sum of eigenstrains and elastic strains. The elastic strain is related to eigenstress by Hooke's law.

When an eigenstrain is prescribed in a finite subdomain Ω in a homogenous material D (Fig. 3.1) and is zero in the matrix D-Ω, then Ω is called an inclusion. The elastic moduli of the material are assumed to be homogenous when inclusions are under consideration.

If a subdomain Ω in a material D has elastic moduli different from those of the matrix, then Ω is called an inhomogeneity. Voids, cracks and precipitates are examples of inhomogeneity, which might also be called an inclusion. Applied stresses will be

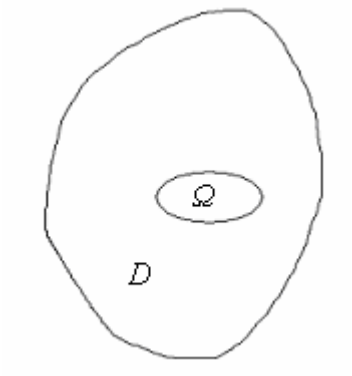

Fig. 3.1 Ellipsoidal Inclusion Ω inside the homogenous matrix

disturbed by the existence of the inhomogeneity. The disturbed stress field will be simulated by an eigenstress field by considering a fictitious eigenstrain ε^*_{ij} in Ω in a homogenous material.

A material containing inhomogeneities is free from any stress field unless a load is applied. On the other hand, a material containing inclusions is subjected to an internal stress (eigenstress) field, even if it is free from all external tractions.

If an inhomogeneity contains an eigenstrain, it is called an inhomogeneous inclusion. Most of the precipitates in alloys and martensites in phase transformation are inhomogeneous inclusions. Eigenstrains inside these inhomogeneous inclusions are misfit and phase transformation strains [8].

J. D. Eshelby first pointed out that the stress disturbance in an applied stress according to the presence of an inhomogeneity can be simulated by eigenstresses caused by an inclusion when eigenstrain is chosen properly. This equivalency will be called the equivalent inclusion method.

3.2.1 The Inhomogeneity Problem

An ellipsoidal region in a solid has elastic constants differing from those of remainder. If, in particular, the constants are zero within the ellipsoid the case is cavity. How is an applied stress, uniform at large distance, disturbed by this inhomogeneity?

The strain in the inclusion or inhomogeneity may be found explicitly in terms of tabulated elliptic integrals. The elastic field at large distance is also easy to determine. The field at intermediate points is more complex, but for many purposes, it is not necessary to know it. In fact, knowing only the uniform strain inside the ellipsoid, one can find the following items of physical or engineering interest:

i. The elastic field far from an inclusion.
ii. The interaction energy of the elastic filed of the inclusion with another field.
iii. The total strain energy in the matrix and inclusion.
iv. The interaction energy of the elastic field of the inclusion with another elastic field.
v. The elastic field far from an inhomogeneity
vi. All the stress and strain components at the point immediately outside the inhomogeneity. This solves the problem of stress concentration.
vii. The interaction energy of the inhomogeneity with an elastic filed.
viii. The change in gross elastic constants of material when a dilute dispersion of ellipsoidal inhomogeneities is introduced into it.

Problem (i) and (iv) can also be solved for an inclusion of arbitrary shape, (ii) and (iii) if one can evaluate the necessary integrals. Problems (v) to (viii) can only be solved for the ellipsoid [2].

According to Eshelby's solution, nowhere one has to introduce ellipsoidal coordinates, suitable stress functions or match stresses and displacements at an interface. Considering shear transformations and the disturbance of an arbitrary shear stress by an ellipsoidal inclusion gives an easier way to solve this problem by Eshelby.

3.2.2 Equivalent Inclusion Method of Eshelby

Consider an infinitely extended material with the elastic moduli C_{ijkl}, containg an ellipsoidal domain Ω, Fig. 3.1, with the elastic moduli C^*_{ijkl}. The disturbance in an applied stress caused by the presence of this inhomogeneity will be investigated. Denote the applied stress at infinity by σ°_{ij} and the corresponding strain by ε°_{ij}. The stress disturbance and strain disturbance are denoted by σ_{ij} and ε_{ij}, respectively. The total stress (actual stress) is $\sigma^\circ_{ij} + \sigma_{ij}$, and the total strain is $\varepsilon^\circ_{ij} + \varepsilon_{ij}$.

Hooke's law is written as

$$\sigma^\circ_{ij} + \sigma_{ij} = C^*_{ijkl}(\varepsilon^\circ_{kl} + \varepsilon_{kl}) \qquad \text{in } \Omega, \tag{3.1}$$

$$\sigma^\circ_{ij} + \sigma_{ij} = C_{ijkl}(\varepsilon^\circ_{kl} + \varepsilon_{kl}) \qquad \text{in } D\text{-}\Omega, \tag{3.2}$$

where C_{ijkl} are the elastic moduli (constants) for the matrix and the summation convention for the repeated indices is employed. If an index occurs twice in any one term, summation is taken from 1 to 3. Moreover, the superscript "*" refers to the material property of the inhomogeneity.

The basic idea of the equivalent inclusion method of Eshelby is to substitute for the inhomogeneity a homogeneous inclusion with the same properties as the matrix, but with an eigenstrain. The eigenstrain must be determined such as to produce the same stresses and strains as the former inhomogeneity.

The equivalent inclusion method is used to simulate the stress disturbance using the eigenstress resulting from an inclusion which occupies the space Ω.

Consider an infinitely extended homogeneous material with elastic moduli C_{ijkl} everywhere, containing a domain Ω with the eigenstrain ε^*_{ij}. The eigenstrain, ε^*_{ij} has been introduced here arbitrarily in order to simulate the inhomogeneity problem by the use of the inclusion method. Such eigenstrain is called an equivalent eigenstrain. When this homogeneous material is subjected to the applied strain ε°_{ij} at infinity, the resulting total stress, strain, and elastic strain, respectively, are $\sigma^\circ_{ij} + \sigma_{ij}$,$\varepsilon^\circ_{ij} + \varepsilon_{ij}$, and $\varepsilon^\circ_{ij} + \varepsilon_{ij} - \varepsilon^*_{ij}$ in Ω. Then, Hooke's law yields

$$\sigma^\circ_{ij} + \sigma_{ij} = C_{ijkl}(\varepsilon^\circ_{kl} + \varepsilon_{kl} - \varepsilon^*_{kl}) \qquad \text{in } \Omega, \tag{3.3}$$

$$\sigma^\circ_{ij} + \sigma_{ij} = C_{ijkl}(\varepsilon^\circ_{kl} + \varepsilon_{kl}) \qquad \text{in } D\text{-}\Omega, \tag{3.4}$$

where

$$\sigma^\circ_{ij} = C_{ijkl}\varepsilon^\circ_{kl}. \tag{3.5}$$

The necessary and sufficient condition for the equivalency of the stress and the strain in the above two problems of inhomogeneity and inclusion is

$$C^*_{ijkl}(\varepsilon^\circ_{kl} + \varepsilon_{kl}) = C_{ijkl}(\varepsilon^\circ_{kl} + \varepsilon_{kl} - \varepsilon^*_{kl}) \qquad \text{in } \Omega, \tag{3.6}$$

The quantity ε_{kl} can be obtained as a known function of ε^*_{kl} when the eigenstrain problem in the homogeneous material is solved. Thus, (3.6) determines ε^*_{kl}

for a given ε°_{kl}, in such a manner that the equivalency holds. After obtaining ε^{*}_{kl}, the stress $\sigma^{\circ}_{ij} + \sigma_{ij}$ can be found from (3.1) or (3.4).

If σ°_{ij} is a uniform stress, ε^{*}_{ij} is also uniform in Ω [5]. Then according to Eshelby's theory

$$\varepsilon_{ij} = S_{ijkl}\, \varepsilon^{*}_{kl}\,, \tag{3.7}$$

where S_{ijkl} is the fourth-order *Eshelby tensor* and for both isotropic and anisotropic materials are given in Eshelby's article [2] or in more explicit format in Mura's book [5]. Substitution of (3.7) into (3.6) leads to

$$C^{*}_{ijkl}\,(\varepsilon^{\circ}_{kl} + S_{klmn}\,\varepsilon^{*}_{mn}) = C_{ijkl}\,(\varepsilon^{\circ}_{kl} + S_{klmn}\,\varepsilon^{*}_{mn} - \varepsilon^{*}_{kl}), \tag{3.8}$$

from which the six unknown components of the eigenstrain, ε^{*}_{ij}, are determined.

Consequently the elastic field inside the ellipsoidal shape inhomogeneity can be calculated based on Eshelby's theory. Through this derivation, Eshelby showed that the deformation of an ellipsoidal inclusion embedded in an infinite homogeneous medium, submitted to uniform remote loading, is homogeneous. This result allows the inhomogeneity problem to be dealt with.

CHAPTER 4

EXTENSION OF ESHELBY'S THEORY FOR ELECTRICAL PROBLEM

4.1 Introduction

Along with the widespread application of piezocomposites, how to determine the effects of defects and inclusions on the properties of such materials becomes one of the most important problems in engineering. For this reason, studying the elastic and electric fields inside and outside piezoceramic part of the piezocomposite is necessary, where in this Chapter, the elastic and electric fields inside piezoceramic will be studied.

In addition to the above reason, how to predict the effective constants according to their constituent properties becomes a very important topic in designing of these composites. One way of calculating the effective coefficients is based on the analysis the coupled elastic and electric fields inside the piezoceramic, presented in this Chapter.

This Chapter attempts to obtain the coupled elastic and electric fields of piezoelectric inhomogeneity in an infinite non-piezoelectric matrix; and based on these result obtain the effective constants of the composite.

It is worthwhile to summarize the previous work directly related to the present study. Extension of the well-known Eshelby's ellipsoidal inhomogeneity solution [2] for elasticity to the piezoelectric material has been done in details by Wang [3]. Wang studied the problem of piezoelectric inclusion in an infinite piezoelectric medium via the Green's function technique to find the integral expressions for the strain and electric

fields, but the integral expressions are very complicated, thus the closed-form solution of strain and electric fields are too difficult to obtain. According to this complexity, conclusions drawn based on his formulation are general. He reached the result that all the field variables are uniform inside the inhomogeneity. With the assumption of a non-piezoelectric material for the matrix, the formulation will be simplified comparing to Wang's work.

No electro-mechanical interaction in the matrix material assumption, a non-piezoelectric medium, has been used in many studies to obtain the coupled elastic and electric field of piezoelectric inhomogeneity in a matrix. Fan and Qin [4] analyzed a piezoelectric ellipsoidal inhomogeneity embedded in a non-piezoelectric elastic matrix via the equivalent inclusion method; see Section 3.2.2. They used a simple way to find the elastic and electric fields inside the inhomogeneity. They applied this assumption to partially decouple the original piezoelectric inhomogeneity problem, although the coupling still holds inside the inhomogeneity.

This Chapter is following the Fan and Qin's work, not only because it simplifies the way to calculate the elastic and electric fields inside the inhomogeneity but also because one can apply their result for any shape of inhomogeneity. Based on their result, the effective properties of piezoceramic composite are studied at end of this Chapter.

Motivated by the above mentioned reason, a physical problem shown in Fig.4.1 is investigated in this Chapter, where a linear piezoelectric ellipsoidal inhomogeneity, Ω, is embedded in a homogenous non-piezoelectric medium, D, where the far fields are

exposed with the uniform strain and electric field. With results of this Chapter, one can find the elastic and electric fields of other ellipsoidal shapes inhomogeneity, such as sphere ($a_1 = a_2 = a_3$), cylinder ($a_3 \to \infty$), and penny shape ($a_1 = a_2 >> a_3$) too.

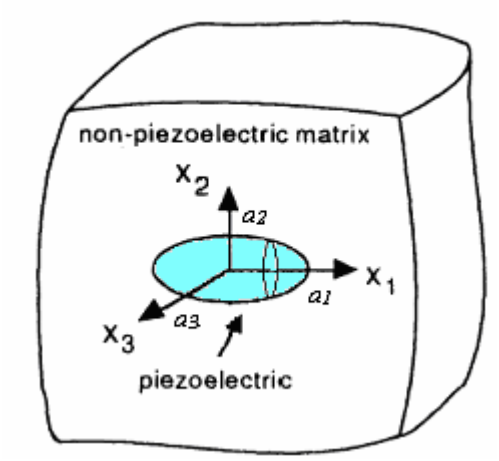

Fig. 4.1 An ellipsoidal piezoelectric inhomogeneity embedded in a non-piezoelectric matrix

In the next section, two inclusion problems will be considered, one is elastic and the other is dielectric. These two inclusion problems are linked by some eigenstrain which corresponds to electro-mechanical coupling terms inside the piezoelectric inhomogeneity. In this connection, the Eshelby's elastic solution and the Eshelby-type solution in a dielectric material play the important roles.

4.2 Equivalent Inclusion Formulation

As is discussed in Section 3.2, a sub-domain with prescribed eigenstrainis called an inclusion, with the same material properties as the matrix; and a subdomain with different material properties, mechanical and electrical, from the remaining material, matrix, is an inhomogeneity. The stress disturbance in an applied stress according to the

presence of an inhomogeneity can be simulated by an eigenstresses caused by an inclusion when an eigenstrain is chosen properly. This equivalency will be called the equivalent inclusion method [4, 8].

Referred to Chapter 2, the constitutive equations for a linear piezoelectric material are

$$\sigma_{ij} = C^*_{ijkl}\,\varepsilon_{kl} - e^*_{ki\,j}\,E_k \qquad \text{in } \Omega, \tag{4.1}$$

$$D_i = e^*_{ikl}\,\varepsilon_{kl} + K^*_{ik}\,E_k \qquad \text{in } \Omega, \tag{4.2}$$

where σ_{ij} and ε_{kl} are the stress and strain, respectively, which are the mechanical field variables, D_i and E_k are the electric displacement and electric field. C^*_{ijkl} is the elastic constants, e^*_{ijk} is the piezoelectric tensor and K^*_{ik} is the permittivity tensor, respectively. The superscript "*" refers to the material property of the piezoelectric inhomogeneity.

Bearing in mind that there is no electro-mechanical coupling in the matrix, the constitutive equations in the matrix are expressed as

$$\sigma_{ij} = C_{ijkl}\,\varepsilon_{kl} \qquad \text{in } D\text{-}\Omega, \tag{4.3}$$

$$D_i = K_{ik}\,E_k \qquad \text{in } D\text{-}\Omega. \tag{4.4}$$

where C_{ijkl} and K_{ik} are the elastic moduli tensor and dielectric permittivity of the matrix. Since there is no coupling between the elastic fields and the electric fields in the matrix, one can consider the terms $e^*_{ki\,j}E_k$ in equation (4.1) and $e^*_{ikl}\,\varepsilon_{kl}$ in equation (4.2) as some kind of eigenstrains [4]. Thus, the original piezoelectric inhomogeneity problem is partially decoupled into the following two equivalent inclusion problems:

4.2.1 The Elastic Equivalent Inclusion Problem

This is a pure elasticity problem. Assume that the far field is loaded with uniform stress. Equation (4.1) is modified as

$$\sigma^{\circ}_{ij} + \sigma_{ij} = C^{*}_{ijkl}(\varepsilon^{\circ}_{kl} + \varepsilon_{kl}) - e^{*}_{kij}(E^{\circ}_{k} + E_{k}), \tag{4.5}$$

or

$$\sigma^{\circ}_{ij} + \sigma_{ij} = C^{*}_{ijkl}(\varepsilon^{\circ}_{kl} + \varepsilon_{kl} - \varepsilon^{E}_{kl}), \tag{4.6}$$

where

$$C^{*}_{ijkl}\varepsilon^{E}_{kl} = e^{*}_{kij}(E^{\circ}_{k} + Ek), \tag{4.7}$$

σ°_{ij} and ε°_{kl} correspond to the uniform far field loading, see equation (3.5).

By employing the equivalent inclusion method, one can convert the inhomogeneity to an inclusion with a certain eigenstrain which depends on the material properties of the inhomogeneity and the far field loading. With this concept, equation (4.6) can be rewritten as

$$\sigma^{\circ}_{ij} + \sigma_{ij} = C_{ijkl}(\varepsilon^{\circ}_{kl} + \varepsilon_{kl} - \varepsilon^{E}_{kl} - \varepsilon^{*}_{kl}). \tag{4.8}$$

Equations (4.6) and (4.8) lead to

$$C^{*}_{ijkl}(\varepsilon^{\circ}_{kl} + \varepsilon_{kl} - \varepsilon^{E}_{kl}) = C_{ijkl}(\varepsilon^{\circ}_{kl} + \varepsilon_{kl} - \varepsilon^{E}_{kl} - \varepsilon^{*}_{kl}), \tag{4.9}$$

where ε^{*}_{kl}, the eigenstrain to be determined, is what one needs to convert the inhomogeneity with elastic constants C^{*}_{ijkl} to an inclusion with elastic constants C_{ijkl} under the applied uniform far field loading. From the famous Eshelby inclusion solution,

$$\varepsilon_{kl} = S_{klmn}(\varepsilon^{E}_{mn} + \varepsilon^{*}_{mn}) = S_{klmn}\,\varepsilon^{**}_{mn}, \tag{4.10}$$

where S_{klmn} is called the Eshelby tensor which was defined in Eshelby's original paper [2] and also in more details [8]. The total eigenstrain ε^{**}_{kl} is then determined by

$$C^*_{ijkl}(\varepsilon^\circ_{kl} + S_{klmn}\,\varepsilon^{**}_{mn} - \varepsilon^E_{kl}) = C_{ijkl}(\varepsilon^\circ_{kl} + S_{klmn}\,\varepsilon^{**}_{mn} - \varepsilon^{**}_{kl}), \tag{4.11}$$

It is apparent that the total eigenstrain, ε^{**}_{kl}, is not only a function of ε°_{kl} but also a function of ε^E_{kl} which is caused by the electro-mechanical coupling of the piezoelectric material [4].

4.2.2 The Equivalent Inclusion Problem in a Dielectric Material

To find the electric field in a dielectric material, the above equivalent inclusion approach is repeated as follows. Let us rewrite equation (4.2) as

$$D^\circ_i + D_i = K^*_{ik}(E^\circ_k + E_k - E^\varepsilon_k), \tag{4.12}$$

where

$$-K^*_{ik}E^\varepsilon_k = e^*_{ikl}(\varepsilon_{kl} + \varepsilon^\circ_{kl}). \tag{4.13}$$

D°_i and E°_k are the known far fields, and E^ε_k is caused by the mechanical-electrical coupling. Furthermore, in terms of the matrix permittivity, K_{ik}, based on equivalent method, the above equation leads to

$$D^\circ_i + D_i = K_{ik}(E^\circ_k + E_k - E^\varepsilon_k - E^*_k), \tag{4.14}$$

Equations (4.12) and (4.14) lead to

$$K^*_{ik}(E^\circ_k + E_k - E^\varepsilon_k) = K_{ik}(E^\circ_k + E_k - E^\varepsilon_k - E^*_k). \tag{4.15}$$

By defining a total *eigen-electric-field*, $E^{**}_k = E^\varepsilon_k + E^*_k$, the electric field disturbance is written as

$$E_k = s_{kl}\,E^{**}_l, \tag{4.16}$$

by using the Green's function technique and extending Eshelby's formulation to electric field equations, s_{kl}, electrostatic Eshelby's tensor, can be defined. One can find the value of this tensor in Chapter 6 for sphere and circular cylinder inhomogeneities.

Then, the equation for E^{**}_k is read as

$$K^*_{ik}(E^\circ_k + s_{kl}\, E^{**}_l - E^{\epsilon}_k) = K_{ik}(E^\circ_k + s_{kl}\, E^{**}_l - E^{**}_k). \tag{4.17}$$

Solving equation (3.17) for E^{**}_k, one will have

$$E^{**}_l = [(K_{im} - K^*_{im})\, s_{ml} - K_{il}]^{-1}[(K^*_{ik} - K_{ik})\, E^\circ_k - K^*_{ik}\, E^{\epsilon}_k]. \tag{4.18}$$

It indicates that the electric field is proportional to the far field load E°_k and the electro-mechanical interaction E^{ϵ}_k.

It is noted that the assumption of the matrix being non-piezoelectric media decoupled the general piezoelectric problem into two inhomogeneity problems. They are dealt with separately by the equivalent inclusion method with interaction terms, ε^E_{kl} and E^{ϵ}_k. Realizing that ε^E_{kl} and E^{ϵ}_k are given by equations (4.7) and (4.13), respectively, more explicit expressions of equations (4.11) and (4.18) are

$$C^*_{ijkl}(\varepsilon^\circ_{kl} + S_{klmn}\, \varepsilon^{**}_{mn}) - e^*_{kij}\, s_{kl}\, E^{**}_l - e^*_{kij}\, E^\circ_k = C_{ijkl}(\varepsilon^\circ_{kl} + S_{klmn}\, \varepsilon^{**}_{mn} - \varepsilon^{**}_{kl}), \tag{4.19}$$

$$E^{**}_l = [(K_{im} - K^*_{im})\, s_{ml} - K_{il}]^{-1}[(K^*_{ik} - K_{ik})E^\circ_k + e^*_{imn}\, S_{mnp}\, \varepsilon^{**}_{pq} + e^*_{ikl}\, \varepsilon^\circ_{kl}]. \tag{4.20}$$

Substituting equation (4.20) into (4.19), the total eigenstrain ε^{**}_{kl} can be obtained explicitly. Furthermore, equations (4.10) and (4.20), with known ε^{**}_{kl}, will provide the strain, $\varepsilon^\circ_{kl} + \varepsilon_{kl}$, and electric field, $E^\circ_k + E_k$, inside the piezoelectric inhomogeneity [4]. Since S_{ijkl} and s_{mn} have been studied extensively for elastic and dielectric media, there are no new integrals introduced in the present formulation. In fact, for some common shapes of the ellipsoidal inhomogeneity, such as spherical, cylindrical and penny shaped

sensors, there are closed form Eshelby tensors available for some anisotropic materials as well as for isotropic materials that will be studied in Chapter 6. Based on the result of this section, the effective properties of the piezoceramic composite can be found. This will be discussed in more details in the next section.

4.3 Analytical Approach to Calculate Effective Material Coefficient of Piezoecramic Composite

As mentioned previously, predicting the effective constants of piezoceramic composite becomes a very important topic in designing of these composites, and one solution of these problems relies on the analysis of the coupled elastic field and electric field of a typical piezoelectric inhomogeneity in a non-piezoelectric medium which has been done in the previous section.

With known strain and electric fields inside an inhomogeneity, the effective elastic, piezoelectric and dielectric constants of piezoelectric composites can be calculated. The effective elastic, piezoelectric and dielectric constants of piezoelectric composites $C^{eff}_{ijkl,}$ e^{eff}_{kij}, K^{eff}_{ik} are defined by the following equations:

$$<\sigma_{ij}> = C^{eff}_{ijkl} <\varepsilon_{kl}> - e^{eff}_{kij} <E_k>, \tag{4.21}$$

$$<D_i> = e^{eff}_{ikl} <\varepsilon_{kl}> + K^{eff}_{ik} <E_k>, \tag{4.22}$$

where < > denotes the volume average. Referring to Wang's study [3] about calculating the effective properties of piezoelectric composite, the equation (4.21) and (4.22) can be written as

$$<\sigma_{ij}> = C_{ijkl} <\varepsilon_{kl}> - e_{kij} <E_k> + v_f C^I_{ijkl} \varepsilon^I_{kl} - v_f e^I_{ki\,j} E^I_k, \tag{4.23}$$

$$<D_i> = e_{ikl} <\varepsilon_{kl}> + K_{ik} <E_k> + v_f e^I_{ikl} \varepsilon^I_{kl} + v_f K^I_{ik} E^I_k, \tag{4.24}$$

where v_f is the volume fraction of inhomogeneity in the piezocomposite and

$$C^{I}_{ijkl} = C^{*}_{ijk\,l} - C_{ijkl}, \tag{4.25}$$

$$e^{I}_{kij} = e^{*}_{kij} - e_{kij}, \tag{4.26}$$

$$K^{I}_{ik} = K^{*}_{ik} - K_{ik}, \tag{4.27}$$

and

$$\varepsilon^{I}_{kl} = \varepsilon_{kl} + \varepsilon^{\circ}_{kl}, \tag{4.28}$$

$$E^{I}_{k} = E_{k} + E^{\circ}_{k}. \tag{4.29}$$

It is noted that, Wang has assumed that the matrix is piezoelectric, in this study the medium is non-piezoelectric, so one can assume zero for the piezoelectric constants of the matrix, *e,* in the above equations. Moreover according to the Gauss theorem, the average value for the stress, strain and electric fields, are equal to applied value of these parameters. This makes it easy to find the effective constants of piezoceramic composite. One can find an example of this solution for different inhomogeneity shapes and volume fraction in Chapter 6.

Although all the effective constants of piezoelectric composite can be obtained in this way, one has to bear in mind that all these analyses have neglected the interactions between inhomogeneities. To obtain a more accurate result, one can use some approximate methods, such as the self-consistent scheme, to consider the interaction [3, 9].

CHAPTER 5

FINITE ELEMENT MODELING

5.1 Introduction

Finite element analysis (FEA) is a numerical method that generates approximate solutions to engineering problems which are often posed in terms of differential equations. The method partitions a structure into simply shaped portions called finite elements, generates an approximation solution for the variable of interest within each element, then combines the approximate solutions. The assemblage of solutions describes the variables of interest for the entire structure.

FEA is used in a variety of engineering applications. Although the first development was for structural analysis, it now solves problems in solid mechanics, fluid mechanics, heat transfer, acoustics and electronics. Using piezoelectric materials is one of the electronic applications in FEA. It can be used to determine full parameters of piezoelectric materials.

In this Chapter, a quick review for modeling in FEA is provided. But the main focus of this Chapter is modeling piezoelectricity with ANSYS, powerful FEA software. Although there are some other powerful FEA programs to model piezoelectricity, the availability of ANSYS dictates the choice of program to be used for the current work.

5.2 Summery of Finite Element Modeling

Using a FEA for solving a problem begins with an essential question, is FEA required to solve this problem? If analytical and experimental solutions are not an option to find the solution, FEA can be used. FEA starts with anticipating a physical behavior of a problem, and planning how the results will be checked to know if they are reasonable. According to the conditions of the problem, an initial FE model will be planned. Now this mode can be used in three FEA phases.

The finite element process is generally divided into the following three distinct phases:

1) *Preprocessing*, to build the FEM model.
2) *Solving*, to solve the equations.
3) *Postprocessing*, to display and evaluate the results.

In the first phase, a proper kind of element, materials properties, model and mesh of the shape, and boundary conditions will be set. It begins by developing a detailed mesh plan that includes the degree of refinement desired in the mesh at all critical locations. The analyst gathers and assembles all the required data and input information for the preprocessor. At this point, the overall geometry of the model section is input with specification of the mesh generation. The actual mesh generation follows, and if the mesh is considered acceptable, the boundary conditions for the enforced displacements are applied. Also, within the preprocessor the load case or cases are input in preparation for the solution runs. These steps complete the preparation of the first model and it is ready to run [10].

Run the analysis program and at the run completion, assuming no errors have been reported, check the output listing file. Access the program's postprocessor, prepare a deformed shape displacement plot and study it for agreement with applied boundary conditions and expected deformations and other results. Examine the stress and other output results through the graphic displays and compare these to boundary conditions values and engineering calculations that were made with approximate equations. These steps provide a good check that the first model was done correctly and approximates the actual behavior, so study of all the results provides further insight into the wanted behaviors.

Evaluation of the results from this first model will show where to refine the model to begin the convergence to an accurate solution. Regions within the model with high stress values and rapid variations as well as regions of low stress are selected for refinement. Reducing the element size in these regions provides refinement. Convergence of results is very important to assure the validity of the analysis.

A serious mistake would be made if only one model was analyzed with no further refinements. Using a finite element program is no guarantee that the results will be accurate although the graphic display may be very convincing. Accurate analyses come about by applying good judgment and good technique to the practice of finite element analysis [10].

Running the second analysis with the refined mesh provides a second solution that may be compared with the first solution to check convergence. Examine the element to element variations for reasonable continuity in the second analysis. Compare

the relative values between the two solutions, and then project or extrapolate to better estimate of the actual solution. Judgment of these comparisons helps decide on further refinements needed to reach the desired convergence.

Rate the final analysis by estimating the accuracy achieved and determining if the important criteria identified at the beginning of the analysis were satisfied. Repeat this cycle until the solution validity is convinced.

In most FEA software, all the above steps can be found. As an example, ANSYS will be studied in more details in next section.

5.3 ANSYS

The ANSYS program has been in commercial use since the 1970s, and has been used extensively in the aerospace, automotive, construction, electronic, manufacturing, nuclear, plastics, oil, and steel industries. In addition, many consulting firms and hundreds of universities use ANYS for analysis, research, and educational use. ANSYS is recognized worldwide as one of the most widely used and capable programs of its type.

The ANSYS computer program is commercial finite element software with the ability to analyze a wide range of different problems. It has excellent pre-processing facilities and is very easy to use. The pre-processing, solution and post-processing drivers are all contained within the same graphical user interface. The analysis capabilities of ANSYS include the ability to solve problems in many engineering fields. As ANSYS has been developed, other special capabilities, such as piezoelectricity and couple filed analysis and design optimization has been added to the program. These

capabilities contribute further to making ANSYS a multipurpose analysis toll to varied engineering disciplines [11].

The main purpose of this section is to solve a piezoelectric problem in ANSYS, as one of the couple field effect.

5.3.1 Piezoelectric Analysis in ANSYS

A coupled-field analysis is an analysis that takes into account the interaction, coupling, between two or more disciplines, fields, of engineering. A piezoelectric analysis, for example, handles the interaction between the structural and electric fields.

As was discussed in Chapter 2, applying a voltage to a piezoelectric material creates a displacement, and vibrating a piezoelectric material generates a voltage. Possible piezoelectric analysis types, available in the ANSYS/Multiphysics or ANSYS/Mechanical products only, are static, modal, harmonic, and transient [11].

Modeling piezoelectricity in ANSYS is almost the same as modeling a simple structural problem. Just some of the steps are different and one needs to follow them to be able to model this kid of materials. The following sections will provide most of these differences. The complete modeling of one piezocomposite will be provided in the next Chapter.

5.3.1.1 Piezoelectric Element Selection

The first important point in piezoelectricity modeling is choosing a right element from couple field elements. *PLANE13, PLANE223, SOLID5, SOLID98, SOLID226* and *SOLID227* are couple field elements and have the ability to be used in piezoelectricity modeling, but this ability should be activated in these elements. The

KEYOPT (1) settings, or *K1* in the interactive mode, activate the piezoelectric degrees of freedom, displacements and voltage. For *PLANE223, SOLID226* and *SOLID227, KEYOPT (1)* should set to 1001 or in the interactive mode, *K1* should set to *piezoelectric*. For *SOLID5* and *SOLID98 KEYOPT (1)* should set to 3 or in the interactive mode, *K1* should set to *UX UY UZ VOLT*. Finally, for *PLANE13 KEYOPT (1)* should set to 7 or in the interactive mode, *K1* should set to *UX UY VOLT*. Remember, *PLANE13, SOLID5*, and *SOLID98* are available in *ANSYS Multiphysics*, *ANSYS Mechanical, ANSYS PrepPost,* and *ANSYS ED* but *PLANE223, SOLID226*, and *SOLID227* are available in *ANSYS Multiphysics, ANSYS PrepPost,* and *ANSYS ED* [11].

ANSYS manual contains a complete library of detailed ANSYS element descriptions, arranged in order by element number. It is the definitive reference for element documentation. One can use this reference to choose a right piezoelectric element from the above list for the modeling.

5.3.1.2 Piezoelectric Material's Properties

As one can find from Chapter 3, a piezoelectric model requires permittivity, or dielectric constants, the piezoelectric matrix, and the elastic coefficient matrix to be specified as material properties.

Because of the difference between manufacturer-supplied data and the format required by ANSYS, conversion of material properties of piezoelectric ceramics has caused many users confusion. This section tries to clarify this point and to provide information on conversion routines.

As mentioned in Chapter 2, the constitutive relationships usually given by manufacturers or published data/reports are in the following form

$$\begin{pmatrix} \varepsilon \\ D \end{pmatrix} = \begin{pmatrix} s^E & d \\ d^T & K^\sigma \end{pmatrix} \begin{pmatrix} \sigma \\ E \end{pmatrix}, \tag{5.1}$$

where σ and ε are the stress and strain vectors, six components are arranged in order of *x, y, z, yz, xz, xy*. *D* and *E* are the electric displacement and the electric field vectors, three components in order of *x, y, z*.

On the other hand, ANSYS requires data in the following form

$$\begin{pmatrix} \sigma \\ D \end{pmatrix} = \begin{pmatrix} C^E - e \\ e^T \quad K^\varepsilon \end{pmatrix} \begin{pmatrix} \varepsilon \\ E \end{pmatrix}, \tag{5.2}$$

where six components of σ and ε are arranged in order of *x, y, z, xy, yz, xz*.

In order to convert the manufacturer's data presented in the form of equation (5.1) to the ANSYS notation presented in the form of equation (5.2), equation (5.1) needs to be based on stress rather than strain. The following manipulations can be performed

$$[\sigma] = [s^E]^{-1}[\varepsilon] - [s^E]^{-1}[d][E], \tag{5.3}$$

$$[D] = [d]^T [s^E]^{-1}[\varepsilon] + \left([K^\sigma] - [d]^T [s^E]^{-1}[d]\right)[E]. \tag{5.4}$$

Moreover

$$[C^E] = [s^E]^{-1}, \tag{5.5}$$

$$[K^\varepsilon] = [K^\sigma] - [d]^T [s^E]^{-1}[d], \tag{5.6}$$

$$[e] = [s^E]^{-1}[d] = [d]^T [s^E]^{-1}. \tag{5.7}$$

Note that the manufacturer's data has a mechanical vector in the form $[x \quad y \quad z \quad yz \quad xz \quad xy]$ whereas ANSYS's mechanical vector is in the form $[x \quad y \quad z \quad xy \quad yz \quad xz]$. One needs to transform the manufacturer's data to the ANSYS input order by switching row and column data for the shear terms. Row and column 4 need to be shifted to 5, and similarly, 5 to 6 and 6 to 4 [maghale tabdyl].

According to the symmetry of transversely isotropic piezoceramic material and poling direction as 3, one can "map" manufacturer data, equations (2.22) and (2.23), to ANSYS data as

$$[C]^E = [s^E]^{-1} = \begin{pmatrix} C_{11} & C_{12} & C_{13} & 0 & 0 & 0 \\ C_{12} & C_{11} & C_{13} & 0 & 0 & 0 \\ C_{13} & C_{13} & C_{33} & 0 & 0 & 0 \\ 0 & 0 & 0 & \frac{C_{11}-C_{12}}{2} & 0 & 0 \\ 0 & 0 & 0 & 0 & C_{44} & 0 \\ 0 & 0 & 0 & 0 & 0 & C_{44} \end{pmatrix}, \tag{5.8}$$

$$[e] = [s^E]^{-1}[d] = \begin{pmatrix} 0 & 0 & e_{31} \\ 0 & 0 & e_{31} \\ 0 & 0 & e_{33} \\ 0 & 0 & 0 \\ 0 & e_{15} & 0 \\ e_{15} & 0 & 0 \end{pmatrix}. \tag{5.9}$$

Moreover, unlike equations in Chapter 2, ANSYS uses the relative permittivity K_r. In order to find this value, one needs to divide the real permittivity used in Chapter 2 by the permittivity of the vacuum K_0,

$$K_r = \frac{K}{K_0}, \tag{5.10}$$

where $K_0 = 8.854 \times 10^{-12}$ *C/Vm*.

Other steps in solving piezoelectric problems are the same as other modeling in ANSYS. For more information about modeling piezoelectricity in ANSYS, one can find one example of this modeling in the next Chapter.

CHAPTER 6

SOLUTIONS AND RESULTS

Piezoelectric composites have been developed in an attempt to improve the properties of monolithic piezoelectric materials, such as lead zirconate titanate (*PZT*), and are of interest for applications such as acoustic transducer, medical imaging and non-destructive evaluation. These materials consist of an active piezoelectric phase and a passive phase, usually a polymer.

As discussed in previous Chapters, finding the elastic and electric fields inside the piezoceramic phase as well as the effective properties of pizocomposites is essential in designing these composites and predicting their behaviors. Two different ways of finding these parameters have been investigated and compared in this thesis, they are an analytical and a numerical approach. In the analytical solution, the coupled elastic and electric fields inside a piezoelectric inhomogeneity embedded in a non-piezoelectric medium can be found based on Eshelby's theory and its extension to the electric field. Based on these elastic and electric fields, the effective properties of the piezocomposite can be found as well. In the numeric approach, ANSYS, commercial finite element software, has been used to model a piezocomposite. Based on this model, the elastic and electric fields can be located inside the piezoceramic phase and also the effective properties of the piezocomposite can be calculated.

Not only the elastic and electric fields as well as the effective coefficients in different approaches have been studied in this thesis but also the effect of both active and passive phases on the overall performance of the piezocomposite materials has been investigated.

In case of the active phase, two piezoceramics with different material properties for two geometric configurations in various volume fractions will be studied. In the analytical solution, these two geometric configurations, sphere and circular cylinder, will be studied in details. But in the numerical solution, only the sphere configuration will be studied in details. In comparing two approaches, the result can be extended to a circular cylinder configuration.

Despite the quite crucial function of the polymer in a piezocomposite, there has been less work focusing on the effect of this polymeric phase on the elastic and electric fields inside the piezoceramic inhomogeneity as well as the effective properties of the composite. When a composite is used in applications such as an ultrasonic transducer with *PZT* piezoceramic, the polymer must effectively couple the ultrasonic energy from a high-acoustic-impedance *PZT* to a low-acoustic-impedance load. Similarly, in the receiving mode, an ultrasonic energy incident on the composite must be effectively transferred to the *PZT*. The properties of the polymer will determine the interaction among the neighboring *PZT* phases and the dynamic behavior of the whole composite thereafter. So in case of the passive phase, two kinds of polymers in various volume fractions will be studied.

6.1 Analytical Solution

In order to calculate the elastic and electric fields inside an inhomogeneity, one needs to calculate ε_{kl} and E_k, with considering ε°_{kl} and E°_k as known quantities, see Sections 4.2.1 and 4.2.1. According to equations (4.10) and (4.16), ε^{**}_{kl} and E^{**}_l need to be defined in order to calculate ε_{kl} and E_k. The eigen-electric-field E^{**}_l can be found from equations (4.20) and with substituting equation (4.20) into (4.19), the total eigenstrain ε^{**}_{kl} can be obtained explicitly. By considering the rule, (2.19), in inverting a tensor to a matrix, (4.19) and (4.20) can be rewritten in matrix notation as

$$[C^*]\ \{[\varepsilon^\circ] + [S]\ [\varepsilon^{**}]\} - [e^*]\ [s]\ [E^{**}] - [e^*]\ [E^\circ]\ = [C]\ \{[\varepsilon^\circ] + [S]\ [\varepsilon^{**}] - [\varepsilon^{**}]\}, \tag{6.1}$$

$$[E^{**}] = \{[K - K^*]\ [s] - [K]\}^{-1}\{[K^* - K]\ [E^\circ] + [e^*]\ [S]\ [\varepsilon^{**}] + [e^*]\ [\varepsilon^\circ]\}, \tag{6.2}$$

and with substituting equation (6.2) into (6.1), $[\varepsilon^{**}]$ can be written as

$$[\varepsilon^{**}] = [G]\ \{[M]\ [\varepsilon^\circ] + [N]\ [E^\circ]\}, \tag{6.3}$$

where

$$[G] = \left\{\left\{[C^* - C] - [e^*]\ [s]\ [H]\ [e^*]^T\right\}\ [S] + [C]\right\}^{-1}, \tag{6.4}$$

$$[H] = \left\{[K - K^*]\ [s] - [K]\right\}^{-1}, \tag{6.5}$$

$$[M] = [C - C^*] + [e^*]\ [s]\ [H]\ [e^*]^T, \tag{6.6}$$

$$[N] = [e^*]\ + [e^*]\ [s]\ [H]\ [K^* - K]. \tag{6.7}$$

All the matrices on the right hand side of the equation (6.3) except $[S]$ and $[s]$ are known from the materials properties of piezoelectric inhomogeneity and non-piezoelectric matrix and the value of applied strain and electric field. By substituting equation (6.3) into (6.2), $[E^{**}]$ can be defined as

$$[E^{**}] = [H]\ \{[O]\ [\varepsilon^{\circ}] + [P]\ [E^{\circ}]\}, \tag{6.8}$$

where

$$[O] = [e^{*}]^{T}\ [S]\ [G]\ [M] + [e^{*}]^{T}, \tag{6.9}$$

$$[P] = [K^{*} - K] + [e^{*}]^{T}\ [S]\ [G]\ [N], \tag{6.10}$$

According to equations (6.3) and (6.8), $[\varepsilon^{**}]$ and $[E^{**}]$ are dependent on both the applied strain, $[\varepsilon^{\circ}]$, and the applied electric field, $[E^{\circ}]$. When stress is applied to a piezocomposite, $[\varepsilon^{\circ}]$ can be found as

$$[\varepsilon^{\circ}] = [C]^{-1}[\sigma^{\circ}]. \tag{6.11}$$

According to equations (4.10) and (4.16), $[\varepsilon]$ and $[E]$ can be defined as

$$[\varepsilon] = [S]\ [G]\{[M]\ [\varepsilon^{\circ}] + [N]\ [E^{\circ}]\}, \tag{6.12}$$

$$[E] = [s]\ [H]\{[O]\ [\varepsilon^{\circ}] + [P]\ [E^{\circ}]\}, \tag{6.13}$$

where $[\varepsilon]$ and $[E]$ are also dependent on both the applied strain and the applied electric field. With known $[\varepsilon]$ and $[E]$, the elastic and electric fields inside the inhomogeneity can be written as:

Elastic fields inside the inhomogeneity

$$\text{Strain} = [\varepsilon] + [\varepsilon^{\circ}], \tag{6.14}$$

according to equations (4.6) and (4.9),

$$\text{Stress} = [\sigma] + [\sigma^{\circ}] = [C]\ \{[\varepsilon^{\circ}] + [\varepsilon] - [\varepsilon^{**}]\}, \tag{6.15}$$

Electric fields inside the inhomogeneity

$$\text{Electrical filed} = [E] + [E^{\circ}], \tag{6.16}$$

according to equation (4.12) and (4.15),

$$\text{Electric displacement} = [D] + [D^{\circ}] = [K]\ \{[E^{\circ}] + [E] - [E^{**}]\}. \qquad (6.17)$$

For some common shapes of the ellipsoidal inhomogeneity, see Fig. 6.1, the closed form of the Eshelby matrices are available for some isotropic materials as well as for anisotropic media. For special shapes of inhomogeneities, such as spherical, cylindrical and penny shaped sensors, [*S*] can be found from the Eshelby's original paper [2] or in more explicitly in Mura's book [8]. This matrix is dependent on Poisson's ratio of the matrix and shape of the inhomogeneity. For the same shapes, the electrostatic Eshelby's matrix [*s*] can be defined from Fan and Qin's paper [4] and this matrix is only dependent on the shape of the inhomogeneity.

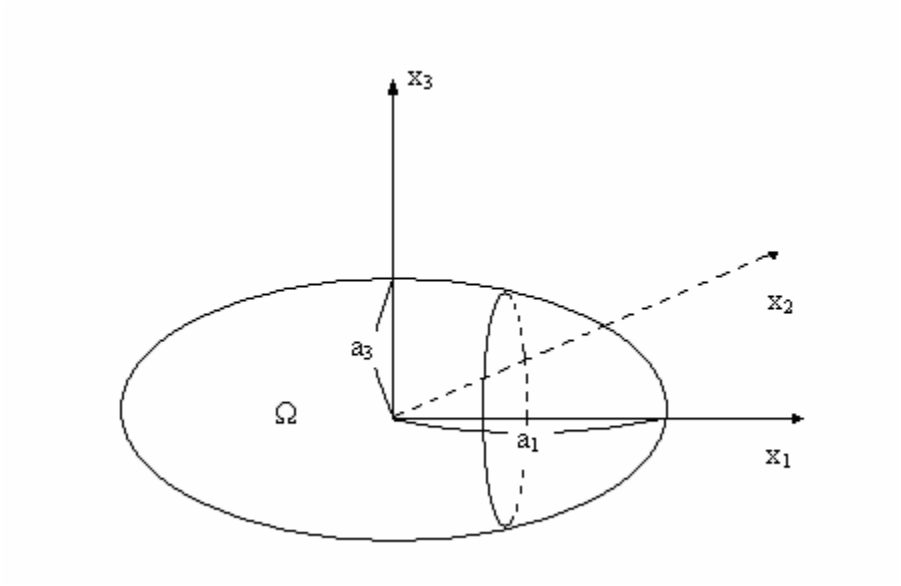

Fig. 6.1 An ellipsoidal inhomogeneity with principal half axes a_1, a_2, and a_3

According to the symmetry of the spherical inhomogeneity in three directions and the circular cylindrical inhomogeneity in two directions, the dependency on the shape has been canceled in [*S*] and [*s*] matrices above. This cancellation can reduce the complexity of the main calculations for the inside's fields as well as effective coefficients. Therefore, these two shapes have been used to be analyzed in this Section.

For a sphere and a circular cylinder, [*S*] and [*s*] can be summarized from those references as:

Sphere, $a_1 = a_2 = a_3 = a$

$$[S] = \begin{pmatrix} A+2B & A & A & 0 & 0 & 0 \\ A & A+2B & A & 0 & 0 & 0 \\ A & A & A+2B & 0 & 0 & 0 \\ 0 & 0 & 0 & B & 0 & 0 \\ 0 & 0 & 0 & 0 & B & 0 \\ 0 & 0 & 0 & 0 & 0 & B \end{pmatrix}, \tag{6.18}$$

where

$$A = \frac{5\nu - 1}{15(1-\nu)}, \tag{6.19}$$

and

$$B = \frac{4 - \nu}{15(1-\nu)}, \tag{6.20}$$

where ν is the Poisson's ratio of the non-piezoelectric matrix,

$$[s] = \begin{pmatrix} 1 & 0 & 0 \\ 0 & 1 & 0 \\ 0 & 0 & 1 \end{pmatrix}. \tag{6.21}$$

Circular cylinder, $a_1 = a_2 = a$ and $a_3 \to \infty$

$$[S] = \begin{pmatrix} C(\frac{3}{4}+D) & C(\frac{1}{4}-D) & C\nu & 0 & 0 & 0 \\ C(\frac{1}{4}-D) & C(\frac{3}{4}+D) & C\nu & 0 & 0 & 0 \\ 0 & 0 & 0 & 0 & 0 & 0 \\ 0 & 0 & 0 & \frac{1}{4} & 0 & 0 \\ 0 & 0 & 0 & 0 & \frac{1}{4} & 0 \\ 0 & 0 & 0 & 0 & 0 & C(\frac{1}{4}+D) \end{pmatrix}, \tag{6.22}$$

where

$$C = \frac{1}{2(1-\nu)}, \tag{6.23}$$

and

$$D = \frac{1-2\nu}{2}, \tag{6.24}$$

where ν is the Poisson's ratio of the non-piezoelectric matrix,

$$[s] = \begin{pmatrix} \frac{1}{2} & 0 & 0 \\ 0 & \frac{1}{2} & 0 \\ 0 & 0 & 0 \end{pmatrix}. \tag{6.25}$$

As mentioned in Section 4.3, with the known strain field, $\varepsilon^{\circ}_{kl} + \varepsilon_{kl}$, and the electric field, $E^{\circ}_k + E_k$, inside an inhomogeneity the effective elastic, piezoelectric and dielectric constants of piezoelectric composites can be calculated. From equations (4.21) through (4.29) in Section 4.3, the effective constants of piezocomposite can be

defined. By assuming a non-piezoelectric matrix and considering the Gauss theorem as well as equation (2.19), equations (4.1), (4.22), (4.23) and (4.24) can be rewritten as

$$[\sigma^\circ] = [C^{eff}]\,[\varepsilon^\circ] - [e^{eff}]\,[E^\circ], \tag{6.26}$$

$$[D^\circ] = [e^{eff}]\,[\varepsilon^\circ] + [K^{eff}]\,[E^\circ], \tag{6.27}$$

$$[\sigma^\circ] = [C]\,[\varepsilon^\circ] + v_f\,[C^* - C]\,[\varepsilon^\circ + \varepsilon] - v_f\,[e^*]\,[E^\circ + E], \tag{6.28}$$

$$[D^\circ] = [K]\,[E^\circ] + v_f\,[e^*]\,[\varepsilon^\circ + \varepsilon] + v_f\,[K^* - K]\,[E^\circ + E]. \tag{6.29}$$

Now, comparing equations (6.26) and (6.28) together, and also (6.27) and (6.29) together, with considering $[\varepsilon]$ and $[E]$ are both dependent on applied strain $[\varepsilon^\circ]$ and applied electric field $[E^\circ]$, can define the effective constants as

$$\left[C^{eff}\right] = [C] + v_f[C^* - C] + v_f[C^* - C]\,[S]\,[G]\,[M] - v_f[e^*]\,[s]\,[H]\,[O], \tag{6.30}$$

$$\left[e^{eff}\right]^T = v_f[e^*]^T + v_f[e^*]^T[S]\,[G]\,[M] + v_f[K^* - K]\,[s]\,[H]\,[O], \tag{6.31}$$

$$\left[K^{eff}\right] = [K] + v_f[e^*]^T[S]\,[G]\,[N] + v_f[K^* - K] + v_f[K^* - K]\,[s]\,[H]\,[P] \tag{6.32}$$

Equations (6.30) through (6.32) show that the effective properties of composites are only dependent on the materials properties of different phases of the composite as well as their volume fractions but are independent of the applied conditions.

With some proper software such as MATLAB, the calculations above can be programmed and inside's fields and the effective properties can be solved straightforward for a specific piezocomposite material.

6.1.1 Results of Analytical Solution

The configuration shown in Fig. 6.2 is used to be analyzed in this Section. A piezocomposite with an infinite polymer matrix in all directions and elliptical

inhomogeneities, randomly distributed in the matrix, is subjected to a far-field hydrostatic stress and a zero far-electric field. One of the main applications of the piezocompoiste is in water or as a biomaterial inside a body; this is the reason to choose hydrostatic state of applied stress in this section. The zero electric field is selected to facilitate the ANSYS modeling in the next Section.

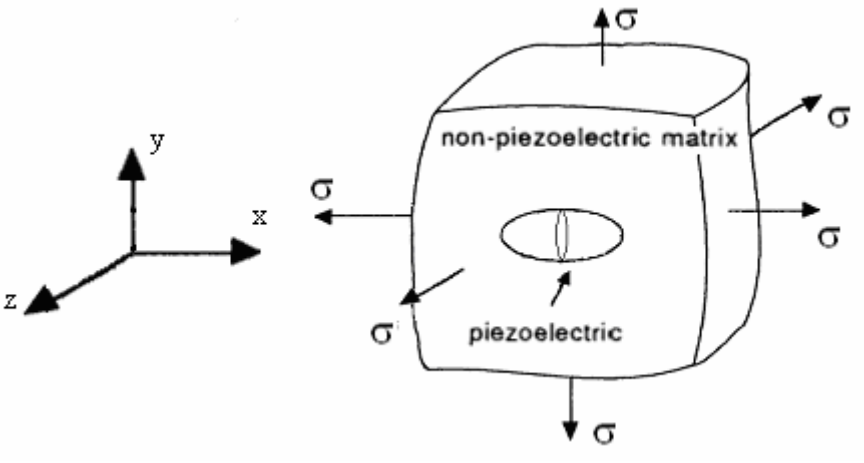

Fig. 6.2 Piezocomposite with infinite polymer matrix and an elliptical inhomogeneity, subjected to a far field hydrostatic stress and zero far electric field, $\sigma_x = \sigma_y = \sigma_z = \sigma$

As an example, two kinds of piezoelectric materials and two kinds of polymers are selected for studying in this Section for two different shapes of inhomogeneity. As a result of this selection, eight different piezocomposites can be produced and analyzed.

For a piezoceramic, the class of *PZT* with a high electromechanical coupling factor, *k*, is conventionally used in the present study. In case of polymers, two commercial available polymers with electronic applications, *Epoxy* and *Unsaturated*

Polyester Resin (UPR), are selected. One can find the properties of these materials in Table 6.1 and Table 6.2.

Table 6.1 Material properties of piezoceramic, C_{ij} $(10^{10}\ N/m^2)$, e_{kl} (C/m^2), K_{ij} $(10^{-10}\ C/Vm)$ [11, 12]

Piezoceramic	C_{11}	C_{33}	C_{44}	C_{12}	C_{13}	e_{13}	e_{33}	e_{15}	K_{11}	K_{33}
PZT4	13.2	11.5	2.60	7.1	7.3	-4.1	14.1	10.5	71.24	58.41
PZT6	16.8	16.3	2.71	6.0	6.0	-0.9	7.1	4.6	36.00	34.00

According to the symmetry described in Chapter 2 for transversely isotropic piezoceramics, only 5 components for the elastic stiffness C, 2 for the permittivity K and 3 for the piezoelectric coefficient e, will be independent as shown in Table 6.1.

Table 6.2 Material properties of polymer matrix, *Young's modulus E (GPa), Poisson's ratio* ν, K $(10^{-10}\ C/Vm)$ [12, 13]

Polymer	E	ν	K
Epoxy	3.4	0.35	0.452
UPR	4.7	0.35	0.328

For isotropic material such as polymers, the stiffness and the permittivity matrices can be calculated as

$$[C]=\frac{E}{(1+\nu)(1-2\nu)}\begin{pmatrix} 1-\nu & \nu & \nu & 0 & 0 & 0 \\ \nu & 1-\nu & \nu & 0 & 0 & 0 \\ \nu & \nu & 1-\nu & 0 & 0 & 0 \\ 0 & 0 & 0 & 1-2\nu & 0 & 0 \\ 0 & 0 & 0 & 0 & 1-2\nu & 0 \\ 0 & 0 & 0 & 0 & 0 & 1-2\nu \end{pmatrix}, \qquad (6.33)$$

$$[K] = \begin{pmatrix} K & 0 & 0 \\ 0 & K & 0 \\ 0 & 0 & K \end{pmatrix}. \tag{6.34}$$

In this section, MATLAB has been used to program all the calculations for different piezocomposites in different volume fractions of the piezoceramic. Based on these calculations, the elastic and electric fields inside the inhomogeneity as well as the effective properties of the piezocomposite can be solved straightforward for the above applied conditions. Table 6.3 and Table 6.4 show the value of elastic and electric fields inside the different shapes of inhomogeneity. According to equations (6.14) to (6.17), the elastic and electric fields inside the inhomogeneity are independent of volume fraction of the piezoceramic, so the values in Table 6.3 and Table 6.4 are valid for any volume fraction. In these Tables, *E* stands for *Epoxy*, *U* for *UPR*, *4* for *PZT4*, *6* for *PZT6, S* for spherical and C for circular cylindrical inhomogeneity. All these calculations are based on $\sigma^{\circ}_1 = \sigma^{\circ}_2 = \sigma^{\circ}_3 = 25Pa$ and $E^{\circ}_i = 0$ as the applied conditions.

Table 6.3 Elastic and electric fields inside the spherical inhomogeneity
ε (10^{-9}), σ (Pa), E (V/m), D (C/m^2)

Piezocomposite	$[\varepsilon]$	$[\sigma]$	$[E]$	$[D]$
E4	$\begin{pmatrix} 0.1316 \\ 0.1316 \\ 0.1266 \\ 0 \\ 0 \\ 0 \end{pmatrix}$	$\begin{pmatrix} 35.4519 \\ 35.4519 \\ 35.4666 \\ 0 \\ 0 \\ 0 \end{pmatrix}$	$\begin{pmatrix} 0 \\ 0 \\ -0.1208 \end{pmatrix}$	$\begin{pmatrix} 0 \\ 0 \\ 0 \end{pmatrix}$
E6	$\begin{pmatrix} 0.1254 \\ 0.1254 \\ 0.1177 \\ 0 \\ 0 \\ 0 \end{pmatrix}$	$\begin{pmatrix} 35.4850 \\ 35.4850 \\ 35.5074 \\ 0 \\ 0 \\ 0 \end{pmatrix}$	$\begin{pmatrix} 0 \\ 0 \\ -0.1795 \end{pmatrix}$	$\begin{pmatrix} 0 \\ 0 \\ 0 \end{pmatrix}$
U4	$\begin{pmatrix} 0.1306 \\ 0.1306 \\ 0.1257 \\ 0 \\ 0 \\ 0 \end{pmatrix}$	$\begin{pmatrix} 35.2062 \\ 35.2062 \\ 35.2262 \\ 0 \\ 0 \\ 0 \end{pmatrix}$	$\begin{pmatrix} 0 \\ 0 \\ -0.1201 \end{pmatrix}$	$\begin{pmatrix} 0 \\ 0 \\ 0 \end{pmatrix}$
U6	$\begin{pmatrix} 0.1245 \\ 0.1245 \\ 0.1170 \\ 0 \\ 0 \\ 0 \end{pmatrix}$	$\begin{pmatrix} 35.2513 \\ 35.2513 \\ 35.2819 \\ 0 \\ 0 \\ 0 \end{pmatrix}$	$\begin{pmatrix} 0 \\ 0 \\ -0.1784 \end{pmatrix}$	$\begin{pmatrix} 0 \\ 0 \\ 0 \end{pmatrix}$

Table 6.4 Elastic and electric fields inside the circular cylindrical inhomogeneity
ε (10^{-9}), σ (Pa), E (V/m), D ($10^{-7}C/m^2$)

Piezocomposite	$[\varepsilon]$	$[\sigma]$	$[E]$	$[D]$
E4	$\begin{pmatrix} -0.635 \\ -0.635 \\ 2.206 \\ 0 \\ 0 \\ 0 \end{pmatrix}$	$\begin{pmatrix} 32.1544 \\ 32.1544 \\ 160.9881 \\ 0 \\ 0 \\ 0 \end{pmatrix}$	$\begin{pmatrix} 0 \\ 0 \\ 0 \end{pmatrix}$	$\begin{pmatrix} 0 \\ 0 \\ 0.3631 \end{pmatrix}$
E6	$\begin{pmatrix} -0.442 \\ -0.442 \\ 2.206 \\ 0 \\ 0 \\ 0 \end{pmatrix}$	$\begin{pmatrix} 31.6677 \\ 31.6677 \\ 360.5666 \\ 0 \\ 0 \\ 0 \end{pmatrix}$	$\begin{pmatrix} 0 \\ 0 \\ 0 \end{pmatrix}$	$\begin{pmatrix} 0 \\ 0 \\ 0.1646 \end{pmatrix}$
U4	$\begin{pmatrix} -0.416 \\ -0.416 \\ 1.596 \\ 0 \\ 0 \\ 0 \end{pmatrix}$	$\begin{pmatrix} 32.0045 \\ 32.0045 \\ 122.7481 \\ 0 \\ 0 \\ 0 \end{pmatrix}$	$\begin{pmatrix} 0 \\ 0 \\ 0 \end{pmatrix}$	$\begin{pmatrix} 0 \\ 0 \\ 0.2591 \end{pmatrix}$
U6	$\begin{pmatrix} -0.282 \\ -0.282 \\ 1.596 \\ 0 \\ 0 \\ 0 \end{pmatrix}$	$\begin{pmatrix} 31.5360 \\ 31.5360 \\ 226.3123 \\ 0 \\ 0 \\ 0 \end{pmatrix}$	$\begin{pmatrix} 0 \\ 0 \\ 0 \end{pmatrix}$	$\begin{pmatrix} 0 \\ 0 \\ 0.1184 \end{pmatrix}$

The effective constants are calculated for different piezocomposites and volume fractions of the piezoceramic. The analytical solution is based on the assumption of no interaction among the inhomogeneities. This assumption is valid for real composites with small volume fractions. With an increase of the volume fraction, the analytical solution is no longer accurate. Therefore, only small volume fractions of the piezoceramic have been considered in this Chapter. Tables 6.5 to 6.8 show the complete matrices of these values at a constant volume fraction of the piezoceramics, $v_f = 0.1$. For other volume fractions, only the independent and non-zero components have been shown in the Appendix A.

Table 6.5 Permittivity matrix for piezocomposite
$[K^{eff}]$ $(10^{-10}\ C/Vm)$

Piezocomposite	$[K^{eff}]^S$	$[K^{eff}]^C$
E4	$\begin{pmatrix} 0.4970 & 0 & 0 \\ 0 & 0.4970 & 0 \\ 0 & 0 & 0.4970 \end{pmatrix}$	$\begin{pmatrix} 0.542 & 0 & 0 \\ 0 & 0.542 & 0 \\ 0 & 0 & 6.411 \end{pmatrix}$
U4	$\begin{pmatrix} 0.3607 & 0 & 0 \\ 0 & 0.3607 & 0 \\ 0 & 0 & 0.3607 \end{pmatrix}$	$\begin{pmatrix} 0.393 & 0 & 0 \\ 0 & 0.393 & 0 \\ 0 & 0 & 6.299 \end{pmatrix}$
E6	$\begin{pmatrix} 0.4967 & 0 & 0 \\ 0 & 0.4967 & 0 \\ 0 & 0 & 0.4967 \end{pmatrix}$	$\begin{pmatrix} 0.540 & 0 & 0 \\ 0 & 0.540 & 0 \\ 0 & 0 & 3.814 \end{pmatrix}$
U6	$\begin{pmatrix} 0.3605 & 0 & 0 \\ 0 & 0.3605 & 0 \\ 0 & 0 & 0.3605 \end{pmatrix}$	$\begin{pmatrix} 0.393 & 0 & 0 \\ 0 & 0.393 & 0 \\ 0 & 0 & 3.702 \end{pmatrix}$

Table 6.6 Effective piezoelectric matrix for piezocomposite
$[e^{eff}]\,(C/m^2)$

Piezocomposite	$[e^{eff}]^S$	$[e^{eff}]^C$
E4	$\begin{pmatrix} 0 & 0 & -0.0002 \\ 0 & 0 & -0.0002 \\ 0 & 0 & 0.0007 \\ 0 & 0.0015 & 0 \\ 0.0015 & 0 & 0 \\ 0 & 0 & 0 \end{pmatrix}$	$\begin{pmatrix} 0 & 0 & -0.0218 \\ 0 & 0 & -0.0218 \\ 0 & 0 & 1.6895 \\ 0 & 0.0027 & 0 \\ 0.0027 & 0 & 0 \\ 0 & 0 & 0 \end{pmatrix}$
U4	$\begin{pmatrix} 0 & 0 & -0.0002 \\ 0 & 0 & -0.0002 \\ 0 & 0 & 0.0007 \\ 0 & 0.0014 & 0 \\ 0.0014 & 0 & 0 \\ 0 & 0 & 0 \end{pmatrix}$	$\begin{pmatrix} 0 & 0 & -0.0300 \\ 0 & 0 & -0.0300 \\ 0 & 0 & 1.6838 \\ 0 & 0.0026 & 0 \\ 0.0026 & 0 & 0 \\ 0 & 0 & 0 \end{pmatrix}$
E6	$\begin{pmatrix} 0 & 0 & -0.00003 \\ 0 & 0 & -0.00003 \\ 0 & 0 & 0.0004 \\ 0 & 0.0015 & 0 \\ 0.0015 & 0 & 0 \\ 0 & 0 & 0 \end{pmatrix}$	$\begin{pmatrix} 0 & 0 & -0.0043 \\ 0 & 0 & -0.0043 \\ 0 & 0 & 0.7546 \\ 0 & 0.0028 & 0 \\ 0.0028 & 0 & 0 \\ 0 & 0 & 0 \end{pmatrix}$
U6	$\begin{pmatrix} 0 & 0 & -0.00003 \\ 0 & 0 & -0.00003 \\ 0 & 0 & 0.0004 \\ 0 & 0.0014 & 0 \\ 0.0014 & 0 & 0 \\ 0 & 0 & 0 \end{pmatrix}$	$\begin{pmatrix} 0 & 0 & -0.0059 \\ 0 & 0 & -0.0059 \\ 0 & 0 & 0.7535 \\ 0 & 0.0027 & 0 \\ 0.0027 & 0 & 0 \\ 0 & 0 & 0 \end{pmatrix}$

Table 6.7 Effective stiffness matrix for piezocomposite
$[C^{eff}]$ (GPa)

Piezocomposite	$[C^{eff}]^S$
E4	$\begin{pmatrix} 6.3049 & 3.2873 & 3.2814 & 0 & 0 & 0 \\ 3.2873 & 6.3049 & 3.2814 & 0 & 0 & 0 \\ 3.2814 & 3.2814 & 6.3120 & 0 & 0 & 0 \\ 0 & 0 & 0 & 3.3710 & 0 & 0 \\ 0 & 0 & 0 & 0 & 3.3710 & 0 \\ 0 & 0 & 0 & 0 & 0 & 3.3037 \end{pmatrix}$
U4	$\begin{pmatrix} 8.6845 & 4.5362 & 4.5252 & 0 & 0 & 0 \\ 4.5362 & 8.6845 & 4.5252 & 0 & 0 & 0 \\ 4.5252 & 4.5252 & 8.6978 & 0 & 0 & 0 \\ 0 & 0 & 0 & 4.5613 & 0 & 0 \\ 0 & 0 & 0 & 0 & 4.5613 & 0 \\ 0 & 0 & 0 & 0 & 0 & 4.4496 \end{pmatrix}$
E6	$\begin{pmatrix} 6.3179 & 3.2805 & 3.2801 & 0 & 0 & 0 \\ 3.2805 & 6.3179 & 3.2801 & 0 & 0 & 0 \\ 3.2801 & 3.2801 & 6.3202 & 0 & 0 & 0 \\ 0 & 0 & 0 & 3.3220 & 0 & 0 \\ 0 & 0 & 0 & 0 & 3.3220 & 0 \\ 0 & 0 & 0 & 0 & 0 & 3.4190 \end{pmatrix}$
U6	$\begin{pmatrix} 8.7087 & 4.5237 & 4.5230 & 0 & 0 & 0 \\ 4.5237 & 8.7087 & 4.5230 & 0 & 0 & 0 \\ 4.5230 & 4.5230 & 8.7130 & 0 & 0 & 0 \\ 0 & 0 & 0 & 4.4796 & 0 & 0 \\ 0 & 0 & 0 & 0 & 4.4796 & 0 \\ 0 & 0 & 0 & 0 & 0 & 4.6432 \end{pmatrix}$

Table 6.8 Effective stiffness matrix for piezocomposite
$[C^{eff}]$ (GPa)

Piezocomposite	$[C^{eff}]^C$
E4	$\begin{pmatrix} 6.165 & 3.264 & 3.310 & 0 & 0 & 0 \\ 3.264 & 6.165 & 3.310 & 0 & 0 & 0 \\ 3.310 & 3.310 & 11.634 & 0 & 0 & 0 \\ 0 & 0 & 0 & 3.319 & 0 & 0 \\ 0 & 0 & 0 & 0 & 3.319 & 0 \\ 0 & 0 & 0 & 0 & 0 & 3.152 \end{pmatrix}$
U4	$\begin{pmatrix} 8.500 & 4.503 & 4.565 & 0 & 0 & 0 \\ 4.503 & 8.500 & 4.565 & 0 & 0 & 0 \\ 4.565 & 4.565 & 13.686 & 0 & 0 & 0 \\ 0 & 0 & 0 & 4.500 & 0 & 0 \\ 0 & 0 & 0 & 0 & 4.500 & 0 \\ 0 & 0 & 0 & 0 & 0 & 4.279 \end{pmatrix}$
E6	$\begin{pmatrix} 6.174 & 3.261 & 3.208 & 0 & 0 & 0 \\ 3.261 & 6.174 & 3.208 & 0 & 0 & 0 \\ 3.208 & 3.208 & 18.386 & 0 & 0 & 0 \\ 0 & 0 & 0 & 3.275 & 0 & 0 \\ 0 & 0 & 0 & 0 & 3.275 & 0 \\ 0 & 0 & 0 & 0 & 0 & 3.225 \end{pmatrix}$
U6	$\begin{pmatrix} 8.517 & 4.499 & 4.426 & 0 & 0 & 0 \\ 4.499 & 8.517 & 4.426 & 0 & 0 & 0 \\ 4.426 & 4.426 & 20.385 & 0 & 0 & 0 \\ 0 & 0 & 0 & 4.427 & 0 & 0 \\ 0 & 0 & 0 & 0 & 4.427 & 0 \\ 0 & 0 & 0 & 0 & 0 & 4.406 \end{pmatrix}$

6.2 Numerical Solution

For the numeric approach, ANSYS, commercial finite element software, has been used to find the elastic and electric fields inside the inhomogeneity as well as the effective properties of piezocomposite.

Although with reviewing Chapter 5, one can model piezoelectricity in ANSYS, this modeling has been reviewed in more details for the piezocomposites in the next Section.

6.2.1 Modeling a Piezocomposite in ANSYS

The problem configuration is the same as in Fig. 6.2. Unlike the analytical solution, the matrix in the ANSYS model is no longer infinite. As a result, a piezocomposite with a finite polymer matrix and elliptical inhomogeneities is subjected to a hydrostatic stress and zero electric field.

With 2-D modeling and selecting plane strain option for the elements, the infinite matrix assumption can be modeled the same as analytical solution. However finding the elastic and electric fields inside the inhomogeneity in all directions as well as all the effective properties needs three dimensional finite element modeling. So finite matrix will bring the first reason for the difference between the results of ANSYS and analytical solution. This difference is independency of the elastic and electric fields inside the inhomogeneity to volume fraction of inhomogeneity in the case of analytical solution and dependency in the case of ANSYS model.

As an example, the same piezoelectric and polymer material as in Section 6.1.1 are selected to study in this Section for only one geometric configuration of inhomogeneity, i.e. sphere. As a result of this selection, four different piezocomposite can be modeled and analyzed.

In order to model the piezocomposite, the actual piezocomposite, with randomly distributed inhomogeneities as used in Section 6.1, is replaced by a repeated spherical array of piezoceramic embedded in a homogeneous matrix material of finite dimensions as shown in Fig. 6.3. The regular inhomogeneity array is then reduced to the smallest, fully informative, repeating segment as shown in Fig. 6.3 in the dashed square. This repeating segment is called a unit cell or a representative volume element. In order to change the volume fraction in the unit cell model, one can change the number of the inhomogeneities in constant volume of the unit cell, which will change the square arrangement of the piezoceramic, as shown in Fig. 6.3, to hexagonal or other arrangements or one can change the geometry of the inhomogeneities.

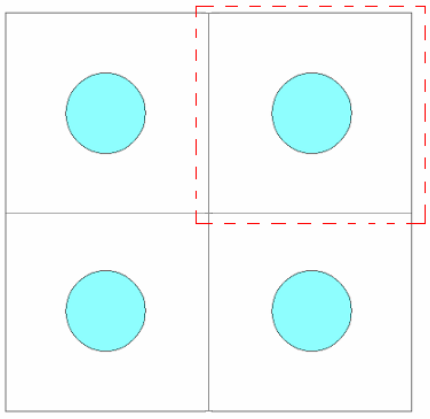

Fig. 6.3 2-D image of unit cell model, square arrangement of sphere piezoceramic

In this section, only one unit cell with just one inhomogeneity is studied. Different volume fractions of the piezoceramic are produced by changing the geometry of the inhomogeneity for the unit length of the cell.

In ANSYS or other FEM software, the first step before modeling a problem is to simplify the problem. Taking the advantages of the symmetry in the above problem, a spherical inhomogeneity embedded at the center of the cell, only one eighth of the unit cell is enough for modeling, see Fig. 6.4. By considering this octant of the problem, the boundary conditions need to be adjusted as shown in Fig 6.5. Now this new problem can be modeled in ANSYS with less complication than the original problem. Start the modeling with *preprocessing* it. It means to select the proper elements, input the materials property, create the geometry, mesh the volume and assign the boundary and loading conditions.

This phase starts with finding the right elements for different parts of the piezocomposite, active and passive parts. For both parts, a block element has the preference over a tetrahedron element; because with block element, a good convergence can be obtained with a small number of elements. According to the existence of sphere, a 20-node block is chosen to cover all the geometry. For the passive part, polymer, the *SOLID95* Element which is a *3-D 20-Node* Structural Solid Element, and for the active part, the piezoceramic, *SOLID226* Element which is *3-D 20-Node* Coupled-Field Solid Element are selected, see Fig. 6.6.

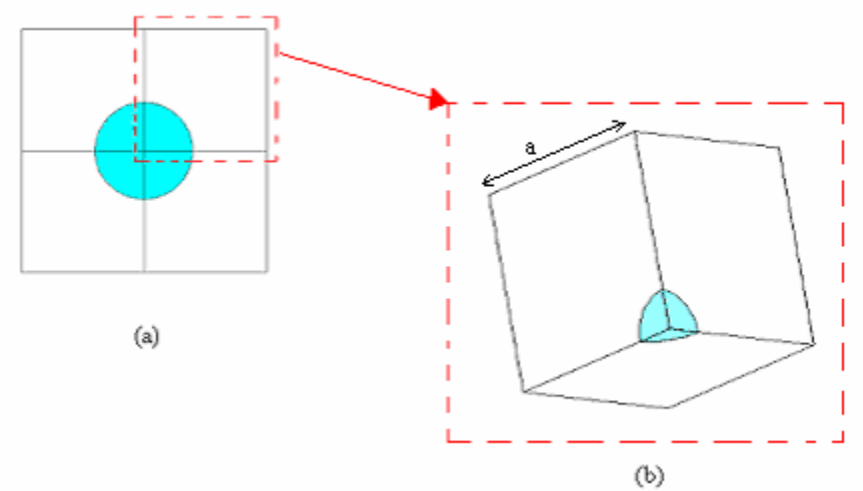

Fig. 6.4 Simplifying the original problem a) 2-D image of unit cell with inhomogeneity at the center b) an octant of the unit cell with spherical inhomogeneity

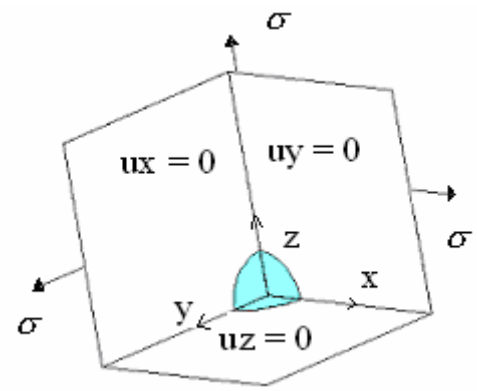

Fig. 6.5 New boundary conditions for the octant of original problem

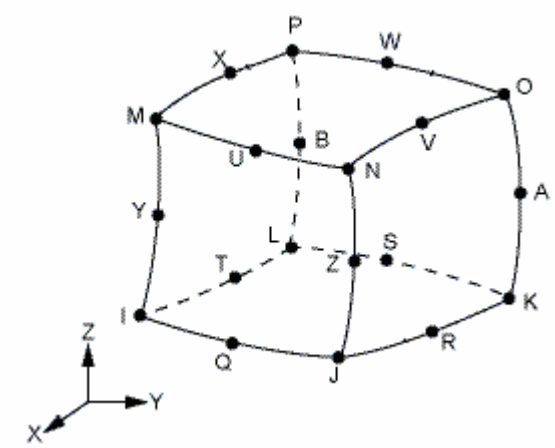

Fig. 6.6 *SOLID95* or *SOLID226* Element

SOLID95 can tolerate irregular shapes without as much loss of accuracy. These brick elements have compatible displacement shapes and are well suited to model curved boundaries. The element is defined by 20 nodes having three degrees of freedom per node, *UX, UY* and *UZ*. The element may have any spatial orientation [11].

SOLID226 has structural, thermal, electrical, thermoelectric, piezoresistive, and piezoelectric capabilities. The element has twenty nodes with up to four degrees of freedom per node, *UX, UY, UZ* and *VOLT*. *SOLID226* has large deflection and stress stiffening capabilities. After selecting this element for modeling the piezoelectricity, go to the option window and select *K1* as *piezoelectric* as shown in Fig 6.7.

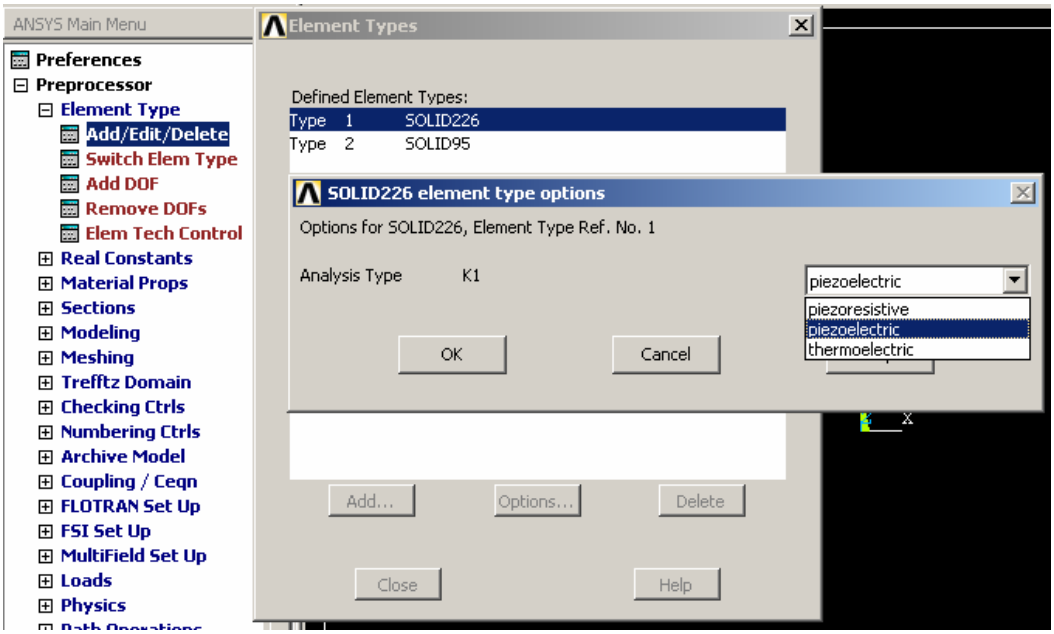

Fig. 6.7 Selecting *K1* as *piezoelectric* for *SOLID226* piezoelectric Element

As discussed in Chapter 5, for the piezoelectric materials, the manufacturer-supplied data needs to be converted to the required format by ANSYS. In order to do this conversion, one needs to read Section 5.31.2 carefully. Equations (5.5), (5.6) and (5.7) are the essential equations for this conversion.

After finding the C^E, e and K^ε, remember that the manufacturer's data has a mechanical vector in the order $[x \quad y \quad z \quad yz \quad xz \quad xy]$ whereas mechanical vector in ANSYS is in the order $[x \quad y \quad z \quad xy \quad yz \quad xz]$ and one needs to transform the manufacturer's data to the ANSYS input order by switching row and column data for the shear terms. Equations (5.8) and (5.9) show the order that is needed for inputting data in ANSYS, also see Fig. 6.9 and 6.10. Again remember ANSYS uses the relative permittivity K_r, see Fig. 6.11.

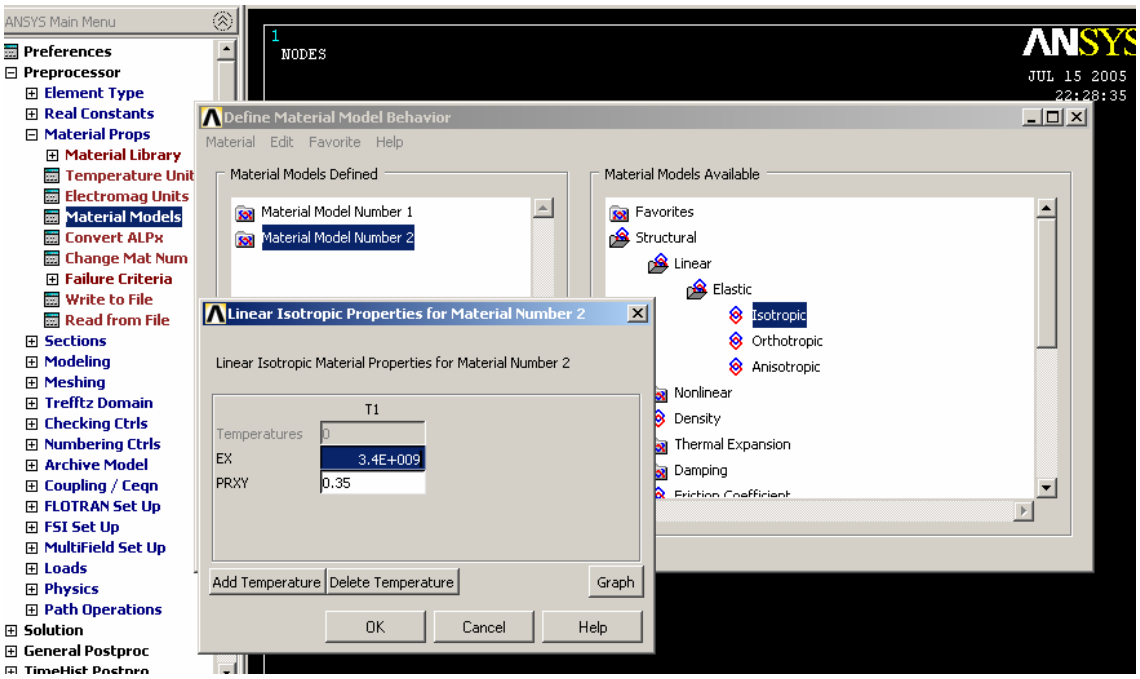

(a)

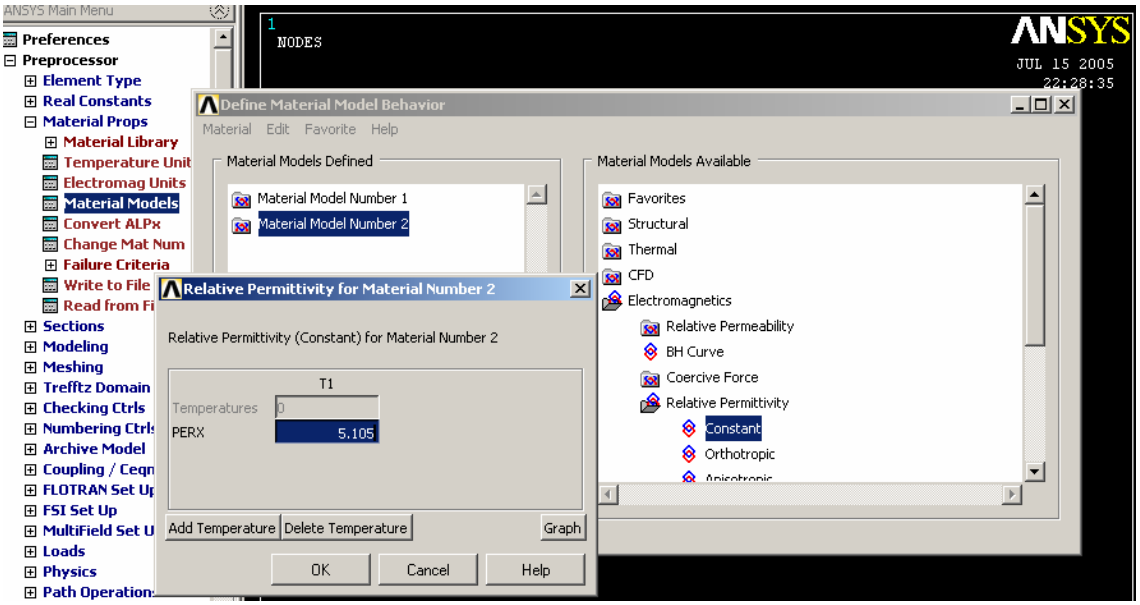

(b)

Fig. 6.8 Inputting material's property of isotropic material (a) Young's Modulus and Poisson's ration of *Epoxy* (b) Relative permittivity K_r of *Epoxy*

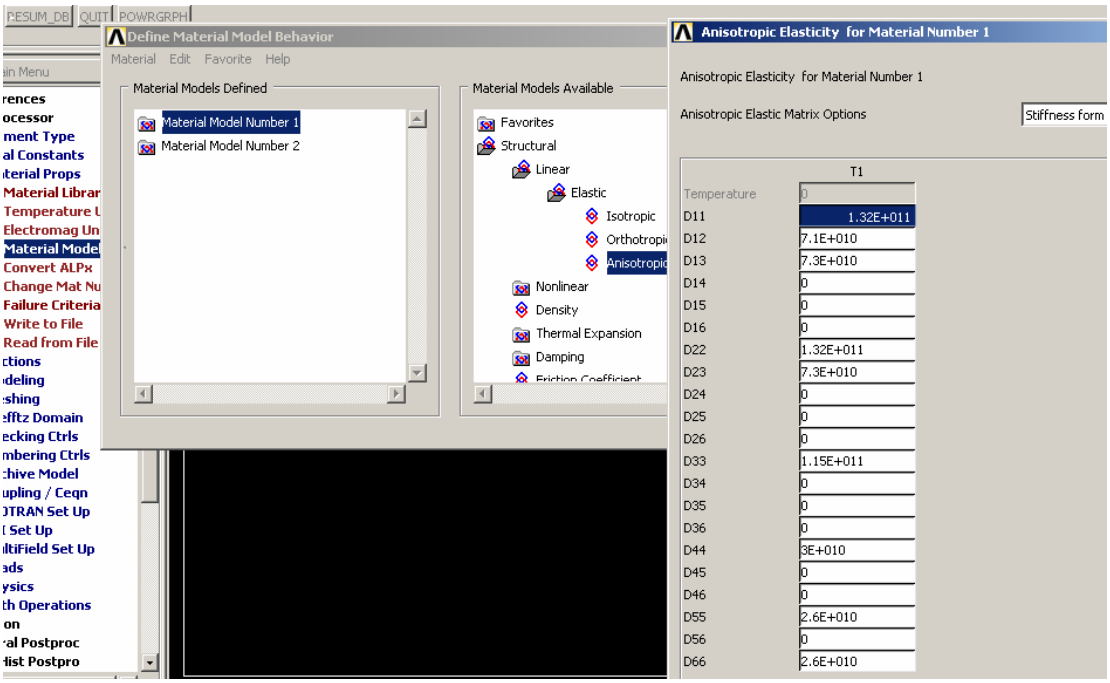

Fig. 6.9 Order of inputting piezoelectric stiffness data, *PZT4*

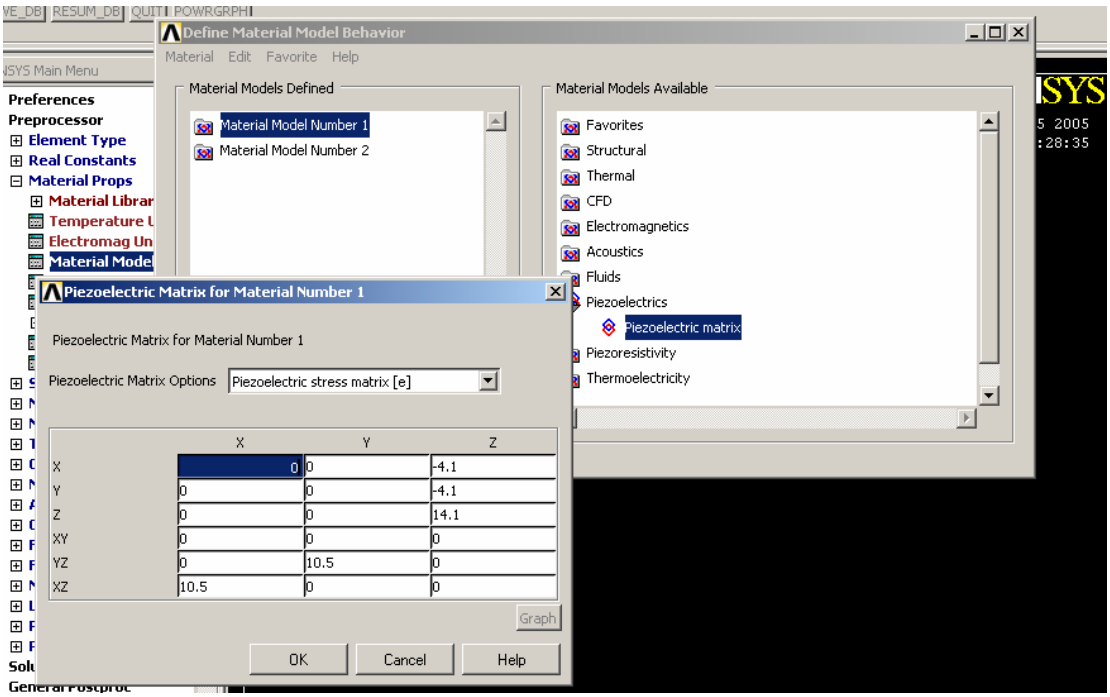

Fig. 6.10 Order of inputting piezoelectricity properties, *PZT4*

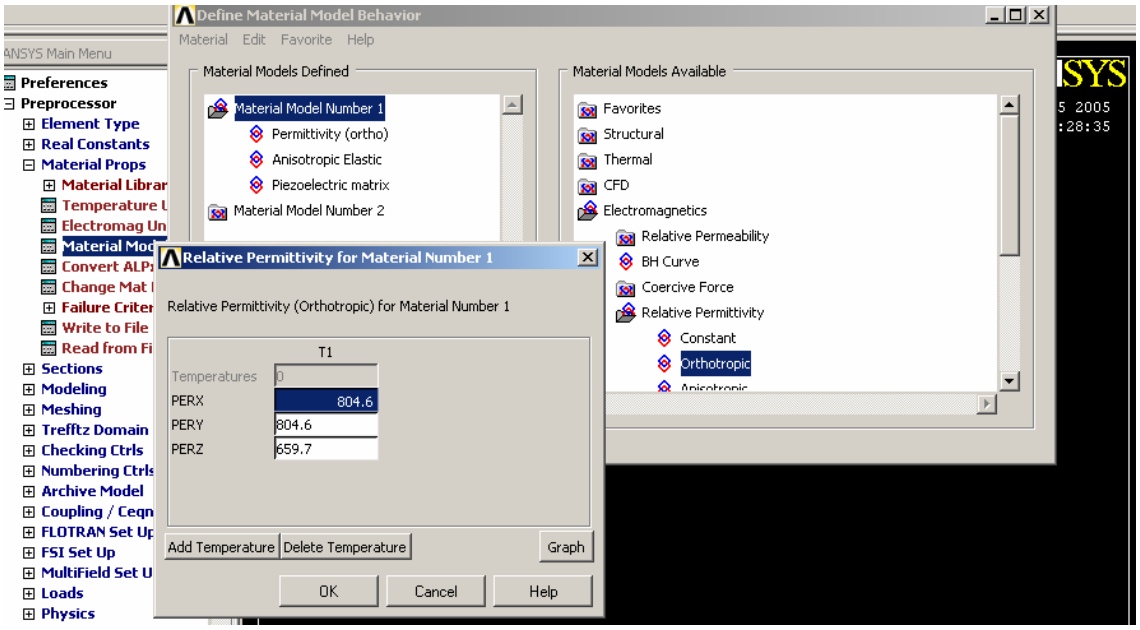

Fig. 6.11 Relative permittivity of piezoelectric, *PZT4*

The next step in the *preprocessing* phase is creating the problem's geometry. As described in the previous Section, only small volume fractions of the piezoceramics have been used in analytical solution. Use the same volume fractions for the ANSYS model. Find the radius of sphere based on this volume fractions and total volume of unit cell as one. As stated before, here increasing the volume fraction of the piezoceramic means increasing the geometry of the inhomogeneity instead of increasing the number of the inhomogeneities. The following equations can be used to calculate the volume fractions. The size of unit cell in Fig. 6.4 (b) has assumed to be unit, $a = 1\ m$.

$$v_f = \frac{volume\ \ of\ \ the\ \ piezoceramic}{volume\ \ of\ \ the\ \ unit\ \ cell}, \tag{6.30}$$

$$v_f = \frac{\frac{4}{3}\pi r^3}{\frac{8}{1}} = \frac{\pi r^3}{6}, \tag{6.31}$$

Based on the above equation and small volume fraction used in analytical solution, the following table shows the different inhomogeneity geometries that need to b modeled.

Table 6.9 Different radii of the spherical inhomogeneity and its corresponding volume fraction

v_f	r
5.23E-7	0.01
5.23E-4	0.1
4.19E-3	0.2
3.35E-2	0.4
26.8	0.8

With different options in the modeling section in ANSYS main menu, one can create the geometry described in Fig. 6.4 (b) and Table 6.9. The only important note is using the *Boolean* operation like *overlap* or *glue* command in order to connect two parts of the piezocomposite together.

The *overlap* commands will join two or more entities to create three or more new entities that encompass all parts of the originals. The end result is similar to an *add* operation, except that boundaries will be created around the overlap zone. Thus, the overlap operation produces a number of relatively uncomplicated regions, as compared to the single relatively complicated region created by the add operation. For this reason,

overlapped entities will often mesh better than added entities. Overlapping is valid only if the overlap region has the same dimensionality as the original entities.

Glue is similar to overlap, except that it applies only to cases in which the intersection between entities occurs at a boundary, and is one dimension lower than the original entities. The entities maintain their individuality, they are not *added*, but they become connected at their intersection.

The Boolean *overlap* and *glue* commands for volumes are as follows:

a) *Main Menu> Preprocessor> Modeling> Operate> Booleans> Overlap> Volumes,*

b) *Main Menu> Preprocessor> Modeling> Operate> Booleans> Glue> Volumes.*

Now it's time for meshing the volume with the selected elements. Remember, before assigning any element and materials property to any volume go to

Main Menu> Preprocessor> Meshing> Mesh Attributes> Default Attribs

and change the default element type number and material number as it should be for the volume that is meshing, polymer volume or piezoceramic volume. Now mesh the volume with the following command as shown Fig. 6. 12:

Main Menu> Preprocessor> Meshing> Mesh> Volume> Free,

and selecting the proper volume. In order to have refiner mesh use the following command:

Main Menu> Preprocessor> Meshing> Modify mesh> Refine at> All.

This study shows that refining the piezoceramic volume will give better result at the end, Fig. 6. 12.

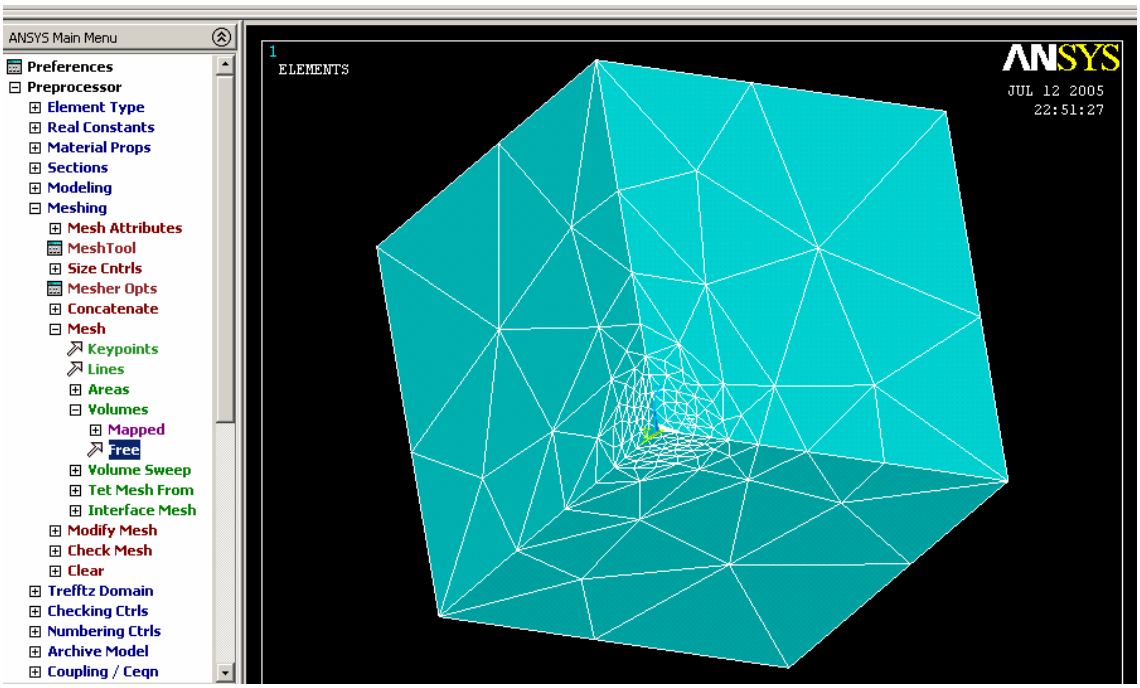

Fig. 6. 12 Meshing the volumes, with refinement in piezoceramic volume

The last step in the *preprocessing* phase is setting the load conditions of the problem as shown in Fig. 6.5. Go the following link

Main Menu> Preprocessor> Loads> Define loads> Apply> Structural> Displacement or Pressure> on Area,

and select the area and apply the boundary conditions as well as loading conditions, Fig. 6.13.

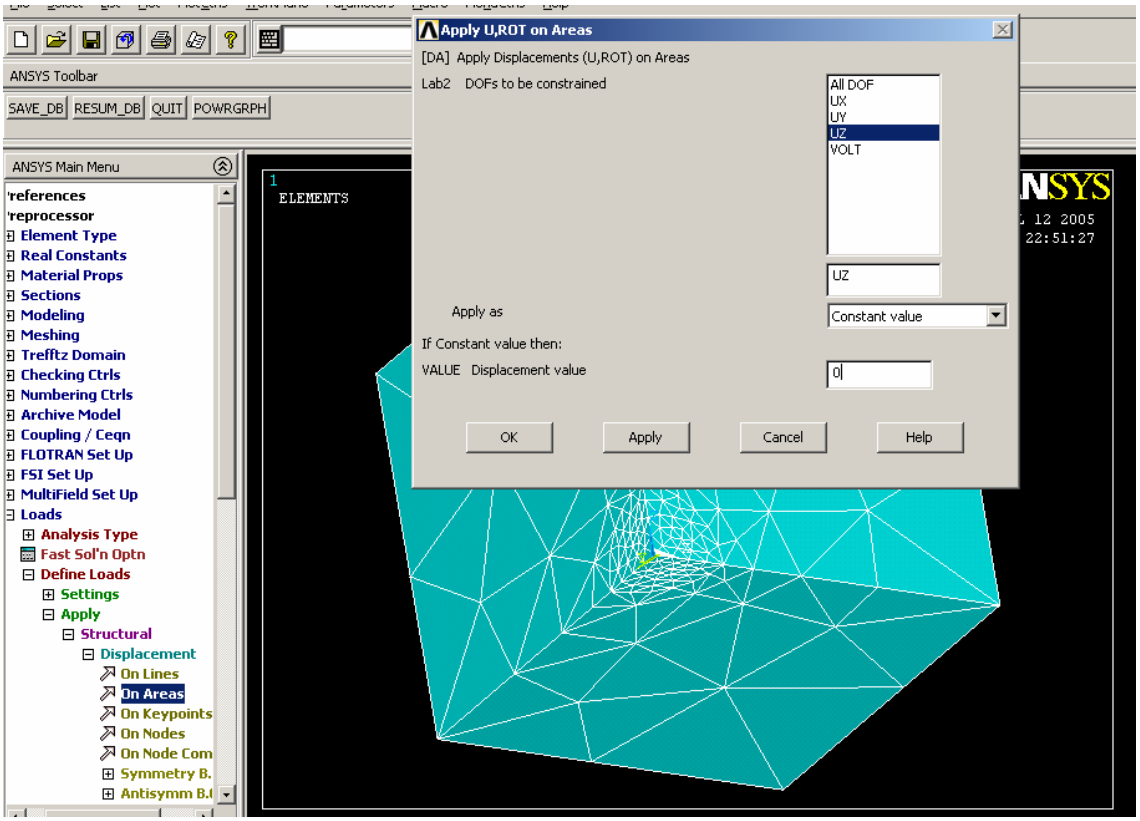

Fig. 6.13 Applying different boundary conditions

Now the model is ready to be solved through the following link:

Main Menu> Preprocessor> Solution> Solve> Current LS

The last phase is the *postprocessing*. In this phase, the results can be displayed and evaluate in a desired way.

The same examples for spherical inhomogeneity as analytical solution have been model here, four different piezocomposites with applied hydrostatic stress and zero electric field at different volume fractions based on Table 6.9. Under these conditions, elastic and electric fields at the center of the piezoceramic have been selected from the output data of ANSYS. Table 6.10 shows the value of elastic and electric fields at the middle

of the piezoceramics for the smallest volume fraction in Table 6.9, v_f = 5.23E-7. According to the symmetry of the sphere, the center of the piezoceramic has been selected as representative of inside points. In these Tables, *E* stands for *Epoxy*, *U* for *UPR*, *4* for *PZT4*, *6* for *PZT6*. Again the applied conditions are $\sigma^\circ_1 = \sigma^\circ_2 = \sigma^\circ_3 = 25Pa$, E°_i = 0 . For the other volume fractions, elastic and electric fields at the center of the piezoceramic have been selected from the output data of ANSYS and gathered in Tables shown in Appendix B.

Table 6.10 Elastic and electric fields at the center of the spherical inhomogeneity
ε (10^{-9}), σ (Pa), E (V/m), D (C/m^2)

Piezocomposite	$[\varepsilon]$	$[\sigma]$	$[E]$	$[D]$
E4	$\begin{pmatrix} 0.133 \\ 0.136 \\ 0.127 \\ -0.58E-4 \\ -0.47E-3 \\ -0.12E-3 \end{pmatrix}$	$\begin{pmatrix} 36.00 \\ 36.00 \\ 35.96 \\ -0.188 \\ -0.014 \\ -0.004 \end{pmatrix}$	$\begin{pmatrix} 3.46E-5 \\ 1.39E-4 \\ -0.1192 \end{pmatrix}$	$\begin{pmatrix} 0 \\ 0 \\ 0 \end{pmatrix}$
E6	$\begin{pmatrix} 0.127 \\ 0.128 \\ 0.119 \\ -0.15E-3 \\ -0.17E-3 \\ -0.19E-3 \end{pmatrix}$	$\begin{pmatrix} 35.98 \\ 36.14 \\ 35.99 \\ -0.005 \\ -0.005 \\ -0.01 \end{pmatrix}$	$\begin{pmatrix} 0.93E-4 \\ 0.14E-3 \\ -0.1808 \end{pmatrix}$	$\begin{pmatrix} 0 \\ 0 \\ 0 \end{pmatrix}$
U4	$\begin{pmatrix} 0.132 \\ 0.135 \\ 0.127 \\ -0.11E-3 \\ -0.55E-4 \\ -0.44E-3 \end{pmatrix}$	$\begin{pmatrix} 35.74 \\ 35.93 \\ 35.71 \\ -0.004 \\ -0.002 \\ -0.013 \end{pmatrix}$	$\begin{pmatrix} 0.32E-4 \\ 0.13E-3 \\ -0.1186 \end{pmatrix}$	$\begin{pmatrix} 0 \\ 0 \\ 0 \end{pmatrix}$
U6	$\begin{pmatrix} 0.126 \\ 0.127 \\ 0.118 \\ -0.14E-3 \\ -0.16E-3 \\ -0.18E-3 \end{pmatrix}$	$\begin{pmatrix} 35.73 \\ 35.88 \\ 35.75 \\ -0.004 \\ -0.005 \\ -0.009 \end{pmatrix}$	$\begin{pmatrix} 0.87E-4 \\ 0.13E-3 \\ -0.1799 \end{pmatrix}$	$\begin{pmatrix} 0 \\ 0 \\ 0 \end{pmatrix}$

To find the effective coefficients in ANSYS, special elastic or electric load, cases with different boundary conditions must be constructed in such a way that for a particular load case only one value in the strain or electric field vector, according to constitutive equation (2.12), is non-zero and all others become zero. Then from one row in equation (2.23) the corresponding effective coefficient can be calculated using the calculated average non-zero value in the strain or electric field vector and the calculated average values in the stress or electrical displacement vector. In this way ones need to find the elastic and electric values for all the nodes and take the average of it. This can be very time consuming and almost impossible. But with using equation (5.1) instead of equation (2.12), the average non-zero value in the strain or electric field value can be found from the data located in the surface of the model, the same surface that stress has been applied, and the calculated average values in the stress or electrical displacement vector will be the same as applied stress and electric filed. The later method can be more convenient to use in ANSYS but in this case stress needs to be applied to the model. Remember with using equation (5.1) to find the effective properties, instead of $[C^{eff}]^E$ and $[e^{eff}]$ and $[K^{eff}]^\varepsilon$, $[S^{eff}]^E$ and $[d^{eff}]$ and $[K^{eff}]^\sigma$ can be found from ANSYS, respectively. Therefore, to compare the results of two approaches, one needs to convert effective matrices found in analytical solution to ANSYS format or vice versa, based on the information stated in Chapter 5.

To make the above calculation more clear, one piezocomposite has been selected and based on the above method the effective stiffness has been calculated in

this Section and compared with result of analytical solution for different volume fractions in the next Section.

As an example, piezocomposite with *Epoxy* polymer matrix and *PZT4* sphere piezoceramic has been selected. The model configuration is the same as shown in Fig. 6.4 (b). In six steps, all the component of compliance matrix can be found with assuming this matrix has the following format as an anisotropic material.

$$[S]^E = \begin{pmatrix} S_{11} & S_{12} & S_{13} & 0 & 0 & 0 \\ S_{21} & S_{22} & S_{23} & 0 & 0 & 0 \\ S_{31} & S_{32} & S_{33} & 0 & 0 & 0 \\ 0 & 0 & 0 & S_{44} & 0 & 0 \\ 0 & 0 & 0 & 0 & S_{55} & 0 \\ 0 & 0 & 0 & 0 & 0 & S_{66} \end{pmatrix}. \tag{6.32}$$

Based on equation (5.1) and assuming the applied electric field is zero, in each step just apply only one stress component and find the corresponding compliance components. As instance if only $\sigma^\circ_x \neq 0$ then

$$\varepsilon_x = S_{11}\sigma^\circ_x, \tag{6.33}$$

$$\varepsilon_y = S_{21}\sigma^\circ_x, \tag{6.34}$$

$$\varepsilon_z = S_{31}\sigma^\circ_x, \tag{6.35}$$

where with considering value of average strain at the surface of the model, one can locate this data from ANSYS output as, ε_i is the average strain in *i* direction found on the plane *i* =1. With 5 more steps, other compliance components can be found and the complete matrix can be converted to stiffness matrix. For one volume fraction, $\nu_f = 0.1$, these values have been gathered in Table 6.11.

Table 6.11 Effective stiffness matrix for *E4* piezocomposite with sphere inhomogeneity $[C^{eff}]$ (GPa)

Piezocomposite	$[C^{eff}]$
E4	$\begin{pmatrix} 5.0540 & 2.5268 & 2.6139 & 0 & 0 & 0 \\ 2.5268 & 5.0540 & 2.6139 & 0 & 0 & 0 \\ 2.6139 & 2.6139 & 5.2097 & 0 & 0 & 0 \\ 0 & 0 & 0 & 1.19775 & 0 & 0 \\ 0 & 0 & 0 & 0 & 1.19775 & 0 \\ 0 & 0 & 0 & 0 & 0 & 2.2457 \end{pmatrix}$

One can find the compliance matrix of other volume fractions for *E4* piezocomposite at Appendix B.

6.3 Evaluation the Results and Discussion

Now based on numerical approach the results can be evaluated, and if there is numerical result for a particular piezocomposite, the results can compare together.

6.3.1 The elastic and electric fields inside the piezoceramic inhomogeneity

These inside's fields for different piezocomposite have been studied based on numerical and analytical solutions. For both approaches the same applied conditions were used, the same hydrostatic stress amount and zero electric field. Results of analytical solution have been studied individually in the following paragraphs, and then its results have been compared to ANSYS results for the same piezocmposites.

First, only consider the found matrices of the inside's fields for one particular piezocomposite, to find the possible relation between the components in different directions. Based on Table (6.3), one can observe for one particular piezocomposite

with sphere ceramic, stress and strain fields inside the spherical inhomogeneity is the same in two directions, *x*, *y* with small difference with the third direction, *z* as shown Fig. 6.11. Because in the case of spherical inhomogeneity, the piezoceramic is completely surrounded by polymer, so in all three directions, an isotropic material transfers the applied stress result in the same stress and strain at the interfaces of the sphere and polymer in all directions. However, the piezoceramic itself is a transversely isotropic material, where in this study the properties of the ceramic is the same in *x* and *y* directions and different in *z* direction. So even though transferred stress is the same at the interfaces of two parts in all directions, but stiffness coefficients are not the same in all these direction. Resulting in the same inside elastic field in *x* and *y* directions and different in *z* direction. With more precise look at the stiffness matrices of *PZT4* and *PZT6*, one can find properties in *z* direction has small difference with the other two directions, resulting in a small difference in the inside elastic field's component in *z* direction compare to the other directions.

One can find the same behavior in piezocomposite in ANSYS model. As an example stress inside the spherical inhomogeneity for *E4S* piezocomposite has been shown in Fig. 6.12 for different volume fractions.

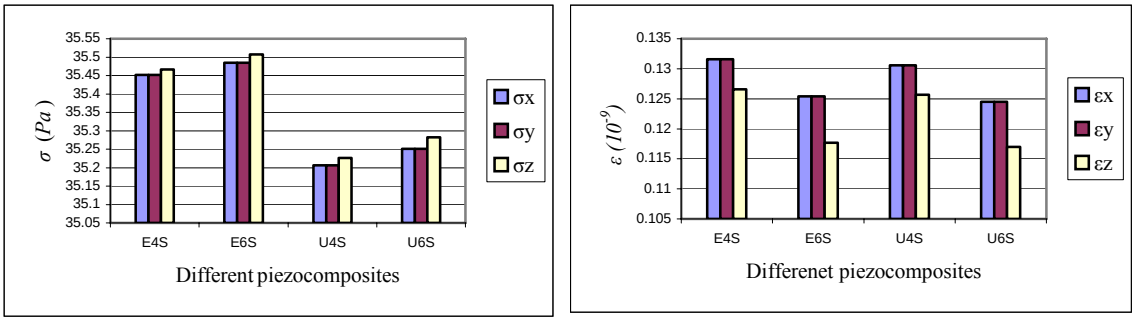

(a) (b)

Fig. 6.11 Elastic fields inside the spherical inhomogeneity for different piezocomposite based on analytical solution, (a) stress field, (b) strain field

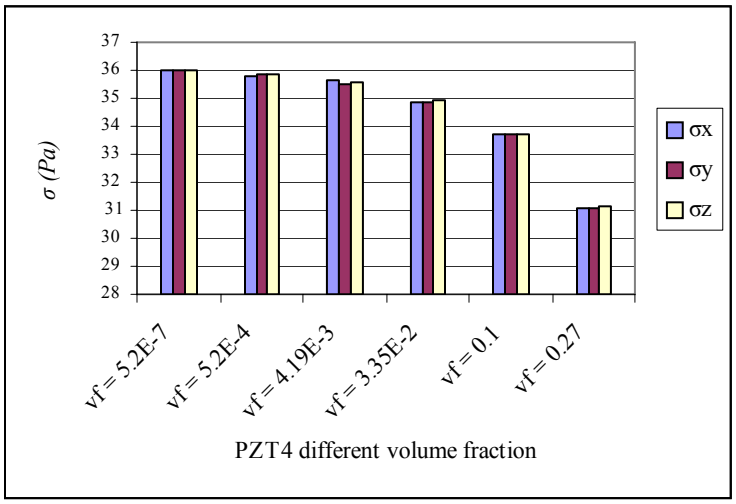

Fig. 6.12 Stress field inside the spherical inhomogeneity for *E4* piezocomposite based on ANSYS modeling

In the case of circular cylinder inhomogeneity, Table 6.4, for one particular piezocomposite, stress and strain fields inside the inhomogeneity is the same in two directions, *x*, *y* with enormous difference with the third direction, *z* as shown Fig. 6.13. In this case, the inhomogeneity is completely surrounded by polymer only in *x* and *y* directions. As stated before in these directions, an isotropic material transfers the

applied stress, resulting in the same transferred stress at interface of two parts of the composite. According to isotropy behavior of the ceramic itself in *x* and *y* directions, the same inside elastic field in *x* and *y* directions will be resulted. However, in the z direction, the piezoceramic has free surface and receiving applied stress directly. Since the stiffness of the piezoceramic is much higher than the polymer in any direction, the stress and strain inside in this direction is much higher than two other directions.

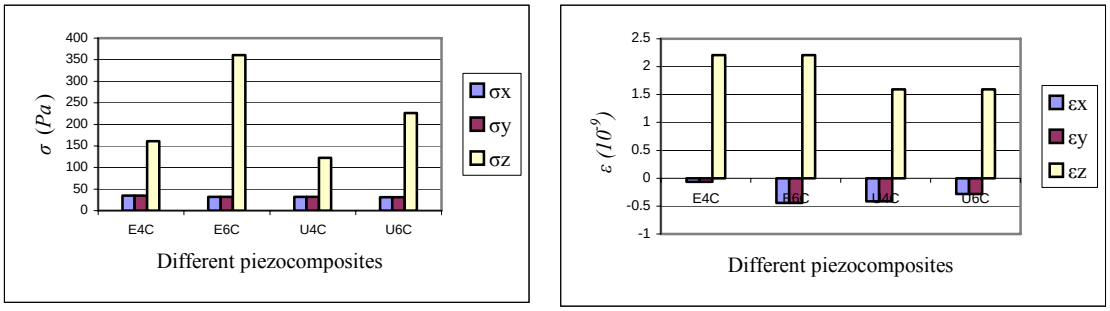

(a) (b)

Fig. 6.13 Elastic fields inside the circular cylindrical inhomogeneity for different piezocomposite based on analytical solution, (a) stress field, (b) strain field

Based on Table (6.3), one can observe for one particular piezocomposite that electric field, *E*, inside the spherical inhomogeneity is zero in two directions, *x*, *y* and non- zero in the third direction, *z*. According to the equation (2.2) and the in the piezoelectricity matrix and value of the e_{15} and poling direction at *z*, because there is no shear stress inside the piezoceramic, there will not be any electric potential at *x* and *y* direction. But according to e_{13} and e_{23} (equal to e_{13}) and e_{33} and normal stresses, non-zero E_z will be resulted in opposite direction of the poling direction. One can find the same

behavior in ANSYS model. As an example electric potential field inside the spherical inhomogeneity for *E4S* piezocomposite has been shown in Fig. 6.14 for different volume fractions in logarithmic scale.

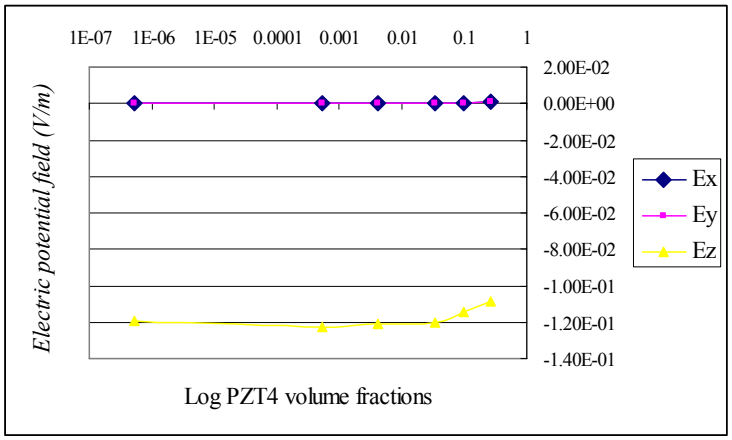

Fig. 6.14 Electric potential field inside the spherical inhomogeneity for *E4* piezocomposite based on ANSYS modeling

As mentioned before, first, elastic and electrical fields inside the piezoceramic inhomogeneity based on analytical solution result is valid for any volume fractions according to its infinite matrix. Second, analytical solution is based on no interaction between the in homogeneities. These assumptions are valid for real composites just for small volume fractions. With increasing the volume fraction, the analytical solution is no longer valid. Therefore only small volume fractions of the piezoceramic have been used in both approaches. Both methods are simulation of real behaviors, so both have their own errors based on how their assumptions produce the model and how they predict the behaviors. In the case of the elastic and electrical fields inside the piezoceramic inhomogeneity, both methods give almost the same result for less than ten

percent volume fraction. Some examples of two approaches comparison have been shown in the Fig. 6.15. In order to show the differences better, logarithmic scale has been used for volume fractions in some graphs.

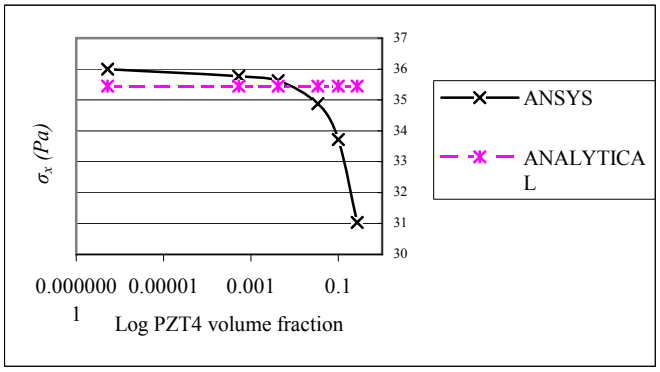

(a)

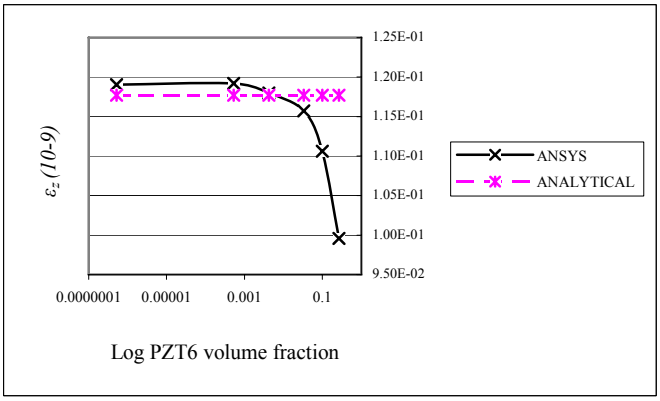

(b)

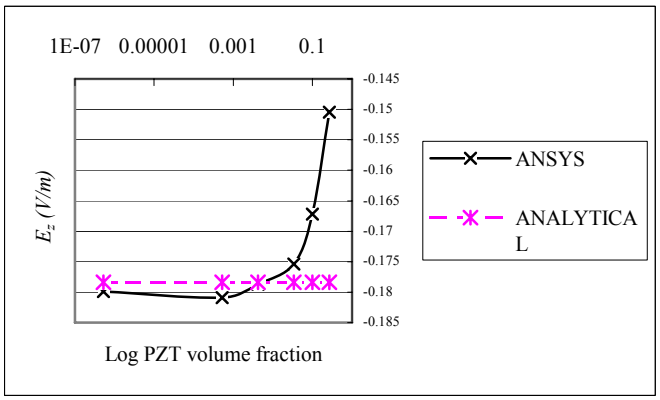

(c)

Fig. 6.15 Comparing elastic and electric fields inside the sphere piezoceramic between the analytical and ANSYS methods (a) σ_x, (b) ε_z, (c) E_z

In addition based on both approaches, effects of three parameters on elastic and electric fields inside the inhomogeneity have been studied. To analyze these effects, in three steps consider two parameters as constant and change the third one as a variable.

First, consider polymer and shape of the in homogeneity are constants and type of the piezoceramic is variable. As an example, consider *E4S* and *E6S* piezocomposites. Although the type of the piezoceramic varies between *PZT4* and *PZT6* the elastic field inside the inhomogeneity is almost the same, Fig. 6.11. The reason is again because of the load-transferring role of the polymer. Both piezoceramics in this case experience the same load at interface of two parts of the composite. The small difference between two composite elastic fields is according to higher stiffness of the *PZT6*, which will cause higher inside stress and lower inside strain. The higher stress inside the in homogeneity will cause the higher electric field, absolute value, in *E6S* according to equation (2.2), Fig. 6.16. In the case of circular cylinder, in *z* direction, polymer has no transferring role. In this direction, higher stiffness of the *PZT6* will cause higher inside stress and lower inside strain, absolute strain, Fig. 6.13. In two other directions, inside stress is almost the same, according to the load- transferring role of the polymer and the small difference is according to small difference in ceramic stiffness matrices. The higher strain inside the homogeneity will cause the higher electric displacement, in *PZT4*, Fig. 6.16.

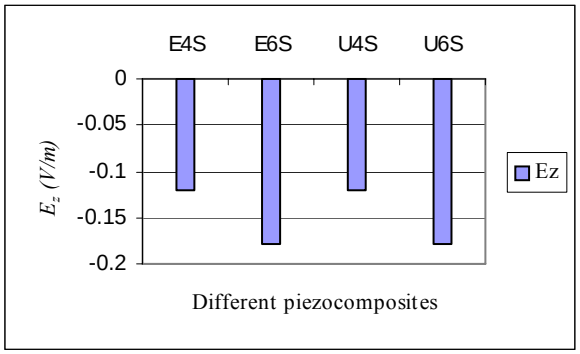

(a)

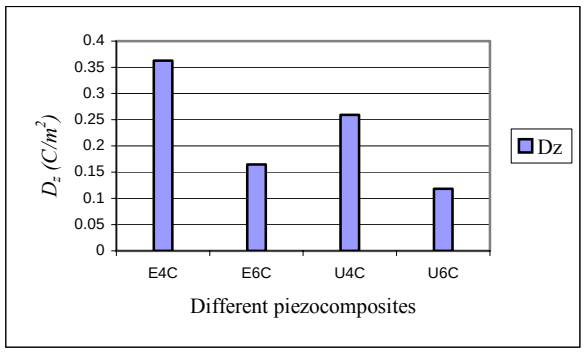

(b)

Fig. 6.16 Electric fields inside (a) the sphere and (b) circular cylinder inhomogeneity for different piezocomposite based on analytical solution

Second, consider piezoceramic and shape of the in homogeneity are constants and type of the polymer is variable. As an example, consider *E4S* and *U4S* piezocomposites. As the type of the polymer changes from *Epoxy* to *UPR* the stress field inside the inhomogeneity will decrease and strain field will increase, Fig. 6.11. Because the *UPR* polymer phase will transfers less load due its higher stiffness than *Epoxy*. As a result, *U4S* interface will receive fewer loads than *E4S*. Higher inside stress in *E4S* will result in higher strain compare to *U4S* with considering the piezoceramic

stiffness is the same for the both composite. The same strain will result in same electrical field in these two composite, Fig. 6.16 (a). Now consider *E4C* and *U4C*. In *x* and *y* directions, the same discussion and result can be conducted as the spherical inhomogeneity, according to the load-transferring role of the polymer, Fig. 6.13. In *z* direction, unlike the prediction, stress inside is not the same for both composite, it seems this parameter is also dependent on characters of the polymer. As a result, again stress at *z* direction is higher in composite with lower polymer stiffness. Again higher strain inside the homogeneity will cause the higher electric displacement, in *E4C*, Fig. 6.16.

Third, consider piezoceramic and polymer material are constants and shape of the inhomogeneity is variable. As an example, consider *E4S* and *E4C* piezocomposites. As stated previously, circular cylinder shape piezoceramic receives applied stress directly in *z* direction, without transferring from the polymer. As the stiffness of the piezoceramic is much higher than polymer, it will result in higher stress in this direction in *E4C* than *E4S*, and higher strain Fig. 6.11 and Fig. 6.13.

From the ANSYS model, the same discussion as above can be conducted based on two parameters, polymer and piezoceramic type. In the constant volume fraction, the same result as analytical solution can be found in ANSYS result for inside's fields, as shown in Fig 6.17 at v_f= 4.199E-3.

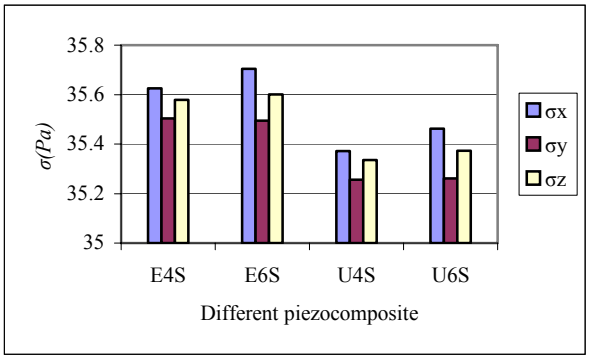

(a)

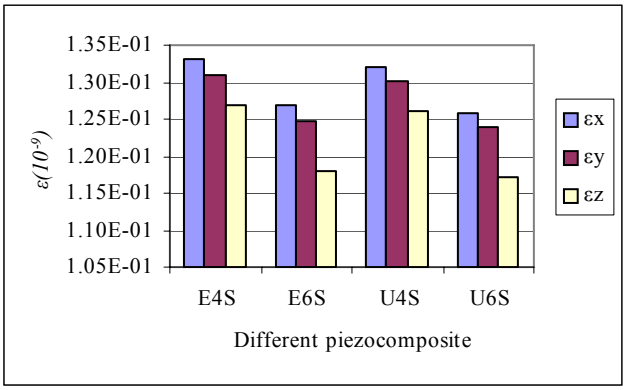

(b)

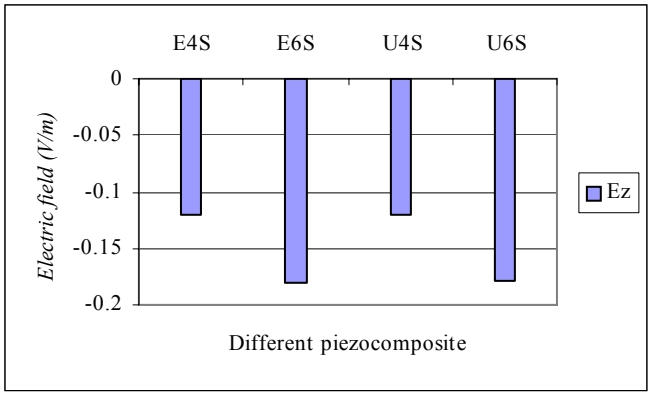

(c)

Fig. 6.17 Elastic and Electric fields for different piezocomposite based on ANSYS method, (a) inside stress, (b) inside strain, (c) inside electric field

6.3.2 The effective properties of the piezocomposites

As studied in details, from both approaches effective properties of the piezocomposite can be calculated. Results of analytical solution for effective properties matrices, show that piezocomposites have isotropic character in two directions, x and y, and anisotropy character in the z direction, valid for both shapes of inhomogeneity in any volume fraction. This anisotropy character is very noticeable in the case of circular cylinder but very small in the case of sphere, Fig. 6.18, Fig. 6.19. and Fig. 6. 20. The polymer matrix is an isotropic material but piezoceramic is a transversely isotropic ceramic with the isotropy in x and y directions and anisotropy in z direction. Piezocomposite has properties between its two parts, based on volume fractions. So it is reasonable that it has anisotropy in z direction according to the existence of piezoceramic with anisotropy in z direction. Spherical inhomogeneity has symmetry in all directions but circular cylinder has longitude shape which cause more anisotropy behavior in properties of the composite. Moreover from the materials properties of *PZT4* and *PZT6* these properties in z direction have small difference with the other two directions, resulting in a small difference in the effective properties of the composite with sphere ceramic in z direction compare to the other directions. In addition with increasing the volume fraction of the sphere the symmetry in shape will be the same so it will not cause much difference between properties in x and z direction, like between C^{eff}_{11} and C^{eff}_{33} Fig. 6.18 (a), or K^{eff}_{11} and K^{eff}_{33} Fig. 6.19 (a), or e^{eff}_{13} and e^{eff}_{33} Fig. 6.20 (a). In the case of circular cylinder inhomogeneity, there is symmetry in plane perpendicular to the axes of the cylinder so there will be isotropy in this plane which

increasing the volume fraction will not change the properties in this plane like C^{eff}_{12} and C^{eff}_{13} because the symmetry will not change, compare C^{eff}_{12} and C^{eff}_{13}, Fig 6.18 (b). But there is anisotropy in cylinder axes direction because of which will be more recognizable with increasing the volume fraction, cause noticeable difference for example between C^{eff}_{11} and C^{eff}_{33} Fig 6.18 (b), or K^{eff}_{11} and K^{eff}_{33} Fig. 6.19 (b), or e^{eff}_{13} and e^{eff}_{33} Fig. 6.20 (b). Moreover, piezocomposites are not transversely isotropic like piezoceramics because their stiffness matrix has six independent components. Remember from Chapter 2 and equation (2.23) that transversely isotropic material has only five independent stiffness components as $C_{66} = \dfrac{C_{11} - C_{12}}{2}$.

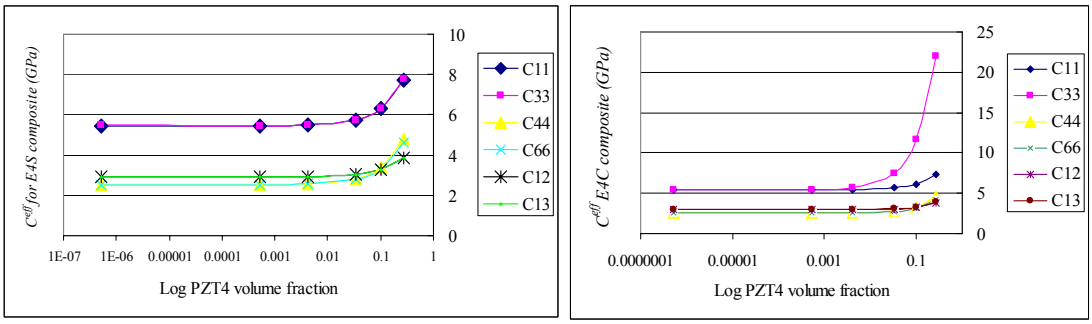

(a) (b)

Fig. 6.18 Difference between C^{eff} components of E4 piezocomposite at different volume fractions (a) sphere piezoceramic and (b) circular cylinder piezoceramic

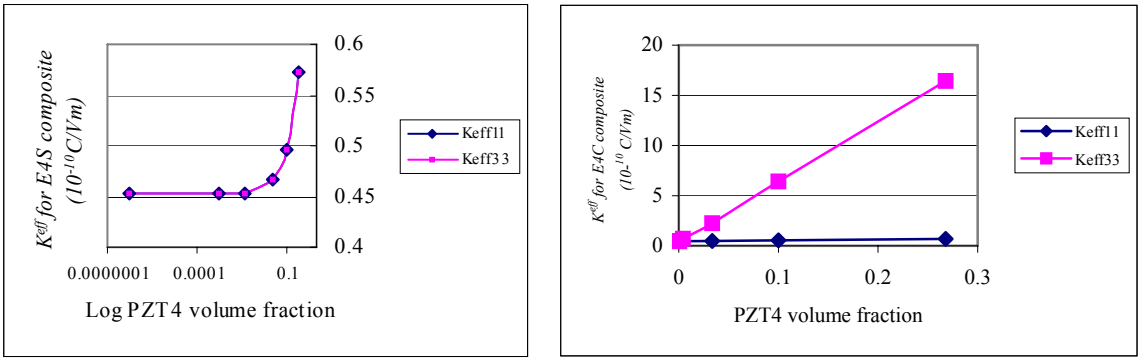

(a) (b)

Fig. 6.19 Difference between K^{eff}_{11} and K^{eff}_{33} for (a) sphere and (b) circular cylinder inhomogeneity

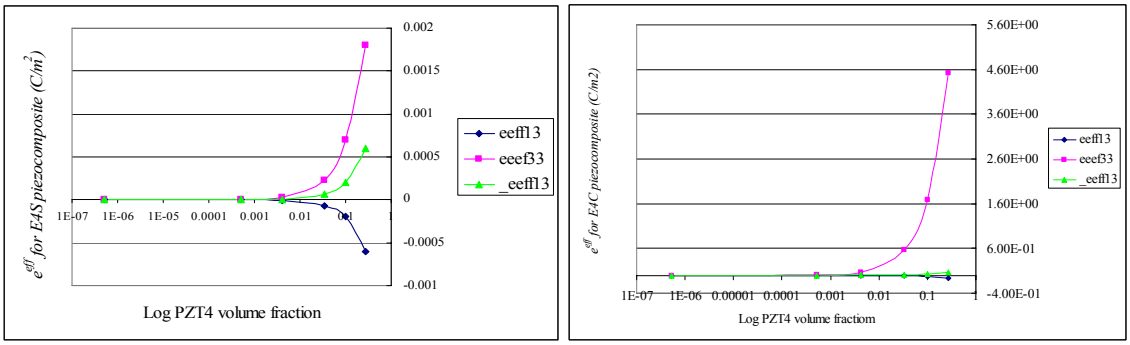

(a) (b)

Fig. 6.20 Difference between e^{eff}_{13} and e^{eff}_{33} for (a) sphere and (b) circular cylinder inhomogeneity

In the case of sphere shape piezoceramic, effective compliance matrices have been calculated based on ANSYS model. From this calculation almost the same evaluation can be report for piezocomposite, Fig. 6.21, isotropy in x and y directions and small anisotropy in the z direction. Also this result has been compared with

numerical calculation and shown in Fig. 6.22. The results are almost the same for low volume fractions but differences will appear in volume fraction higher than ten percent, which the reason was discussed before.

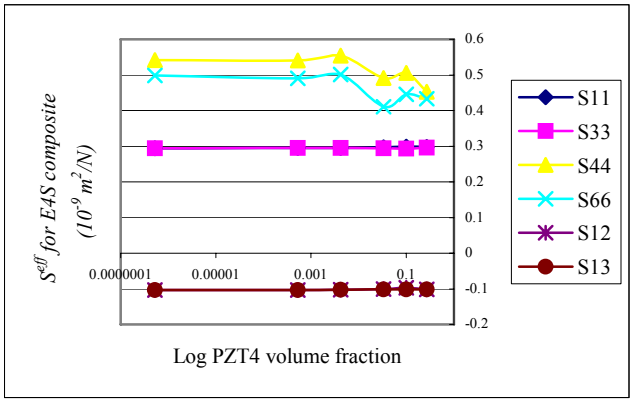

Fig. 6.21 Compliance matrix of *E4S* piezocomposite based on ANSYS model

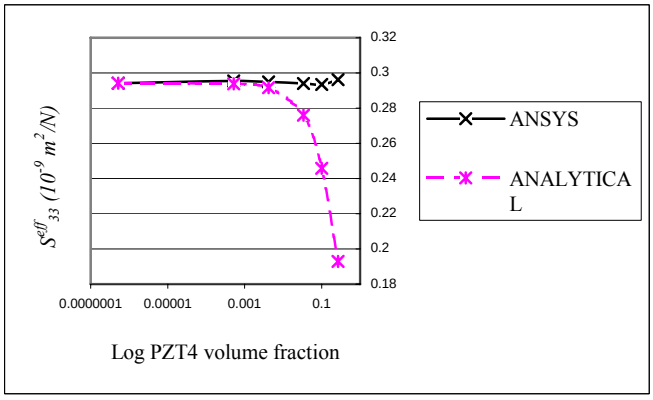

Fig. 6.22 Comparing results of two approaches for compliance matrix of *E4S*

In addition, effects of three parameters on effective parameters of the piezocomposite have been studied here. To analyze these effects, again in three steps consider two parameters as constant and change the third one as a variable for different volume fractions. The result of this comparison shows at low volume fractions of the piezoceramic, the effective properties of the composite is close to the properties of the polymer matrix, with increasing the volume fraction, the effective properties will be change toward the piezoceramic's properties.

As a result, at high volume fraction in the volume fraction range pof this study, piezocomposite with *PZT6* ceramic and *UPR* polymer matrix has higher effective stiffness than piezocomposite with *PZT4* ceramic and *Epoxy* polymer matrix. In the case of piezoelectricity matrix, piezocomposite with *PZT4* ceramic has higher effective piezoelectricity than piezocomposite with *PZT6* ceramic. Remember the polymer has zero piezoelectricity effect. For the effective permittivity, piezocomposite with *PZT4* ceramic and *Epoxy* polymer matrix has higher effective permittivity than piezocomposite with *PZT6* and *UPR*.

The other factor that can be variable is shape of the ceramic. At low volume fractions of the piezoceramic, the effective properties are close to the properties of the polymer matrix without any influence from the shape of the inhomogeneity. With increasing the volume fraction, the effective properties will be change according to shape difference of the piezoceramic. For the effective stiffness, all the components of the matrix such as C^{eff}_{11} are higher for composite with sphere shape piezoceramic except the C^{eff}_{33}, Fig. 6.23. Symmetry difference between these two shapes causes this

result. For the effective piezoelectricity matrix, all the components of the matrix are higher for composite with circular cylinder piezoceramic except the e^{eff}_{33}, Fig. 6.24. For the effective permittivity matrix, all the components of the matrix are higher in the case of the circular cylinder, Fig. 6.25.

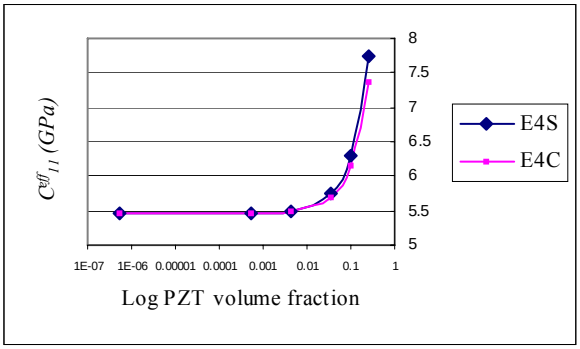

(a)

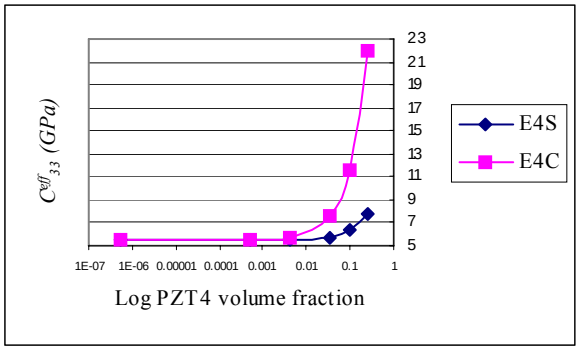

(b)

Fig. 6.23 Difference between effective stiffness matrices of the piezocomposite with different shape of the piezoceramic (a) C^{eff}_{11} (b) C^{eff}_{33}

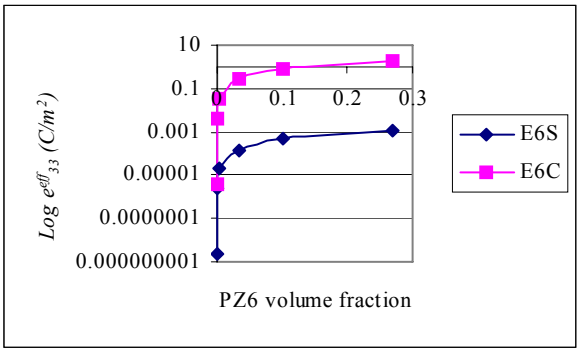

Fig. 6.24 Difference between effective piezoelectricity component e^{eff}_{33} of the piezocomposite with different shape of the piezoceramic

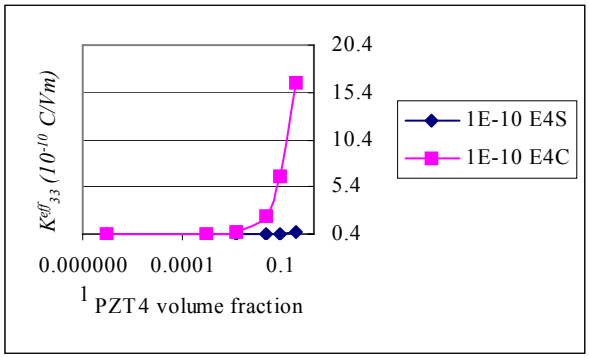

Fig. 6.25 Difference between effective permittivity component K^{eff}_{33} of the piezocomposite with different shape of the piezoceramic

CHAPTER 7

CONCLUSIONS AND RECOMMENDATIONS

The analytical solution based on the extension of Eshelby's theory to piezoelectricity has been purposed in this thesis to calculate the elastic and effective fields inside the piezoceramic inhomogeneity for various piezocomposites. Based on this approach, the effective properties of the piezocomposite have been obtained too. This approach has been tested for different materials and shapes as well as volume fractions. The results for inside's fields and the effective properties were matched with what were expected according to materials property or volume fractions. However, because of the assumptions made for finding the equations in this method, it is only valid for small volume fractions of the inhomogeneities.

Also for these volume fractions, the numerical approach based on ANSYS software has been use to model the same problems as the analytical approach. Based on this model, the elastic and effective fields inside the piezoceramic inhomogeneity for various piezocomposites have been found at the center of these parts. With different boundary conditions, the effective properties of the piezocomposite have been calculated for these FEM models.

The result for both the inside's fields and the effective properties were close to numerical solution for all the piezocomposite only for the small volume fraction of the piezoceramic. For higher volume fraction, more than ten percent of the piezoceramic,

there will be a divergence between the results of two approaches. So as what expected before, the analytical solution based on the extension of Eshelby's theory to piezoelectricity is only valid for small volume fraction of the inhomogeneities.

It is recommended to extent this study for higher volume fraction of the inhomogeneities. For this matter, one needs to consider the interactions among the inhomogeneities, so other methods than the extension of Eshelby's theory to piezoelectricity need to be considered such as the self-consistent scheme, to consider the interactions.

Also, it is recommended to compare the results of this study for lower volume fractions with experimental data. The result of this comparison can be helpful in designing these composite.

APPENDIX A

ANALYTICAL SOLUTION RESULT

Only independent and non-zero components of the effective properties for different piezocomposite at different volume fraction of the piezocomceramic have been shown in the following tables. In these tables, *E* stands for *Epoxy*, *U* for *UPR*, *4* for *PZT4*, *6* for *PZT6, S* for spherical inhomogeneity and *C* for circular cylinder inhomogeneity.

Table A.1 C^{eff}_{11} (*GPa*) from the stiffness matrix

v_f	*E4S*	*E6S*	*U4S*	*U6S*	*E4C*	*E6C*	*U4C*	U6C
5.23E-07	5.4568	5.4568	7.5432	7.5432	5.4568	5.4568	7.5432	7.5432
5.23E-04	5.4612	5.4613	7.5492	7.5493	5.4605	5.4605	7.5482	7.5483
4.19E-03	5.4923	5.4928	7.591	7.592	5.4864	5.4868	7.5833	7.584
3.35E-02	5.7409	5.7452	7.9255	7.9336	5.6939	5.6969	7.8637	7.869
0.1	6.3049	6.3179	8.6845	8.7087	6.165	6.174	8.5	8.517
0.27	7.7293	7.7641	10.601	10.666	7.354	7.378	10.107	10.152

Table A.2 C^{eff}_{33} (*GPa*) from the stiffness matrix

v_f	*E4S*	*E6S*	*U4S*	*U6S*	*E4C*	*E6C*	*U4C*	U6C
5.23E-07	5.468	5.4568	7.5432	7.5432	5.4568	5.4569	7.5432	7.5433
5.23E-04	5.4613	5.4613	7.5493	7.5493	5.4891	5.5245	7.5754	7.6104
4.19E-03	5.4926	5.4929	7.5267	7.5233	5.7154	5.9981	7.8004	8.0809
3.35E-02	5.7432	5.746	7.9299	7.935	7.5258	9.7873	9.6005	11.844
0.1	6.312	6.3202	8.6978	8.713	11.634	18.386	13.686	20.385
0.27	7.7748	7.7702	10.637	10.678	22.009	40.101	24.001	41.953

Table A.3 C^{eff}_{44} (*GPa*) from the stiffness matrix

v_f	*E4S*	*E6S*	*U4S*	*U6S*	*E4C*	*E6C*	*U4C*	*U6C*
5.23E-07	2.5185	2.5185	3.4815	3.4815	2.5185	2.5185	3.4815	3.4815
5.23E-04	2.523	2.5227	3.4865	3.4867	2.5227	2.5225	3.4868	3.4864
4.19E-03	2.5542	2.5522	3.5267	3.5233	2.552	2.5502	3.5241	3.5211
3.35E-02	2.8041	2.7876	3.8432	3.8158	2.7865	2.7719	3.8226	3.798
0.1	3.371	3.322	4.5613	4.4796	3.319	3.275	4.5	4.427
0.27	4.8028	4.6714	6.375	6.156	4.662	4.546	6.211	6.015

Table A.4 C^{eff}_{66} (*GPa*) from the stiffness matrix

v_f	*E4S*	*E6S*	*U4S*	*U6S*	*E4C*	*E6C*	*U4C*	*U6C*
5.23E-07	2.5185	2.5618	3.4815	3.4815	2.5185	2.5185	3.4815	3.4815
5.23E-04	2.5226	2.5232	3.4865	3.4876	2.5218	2.5222	3.4857	3.4863
4.19E-03	2.5512	2.5562	3.522	3.5301	2.545	2.5481	3.5149	3.5202
3.35E-02	2.7815	2.8201	3.8057	3.8706	2.7306	2.7551	3.7486	3.791
0.1	3.3037	3.419	4.4496	4.6432	3.152	3.225	4.279	4.406
0.27	4.6223	4.9313	6.075	6.594	4.215	4.411	5.618	5.958

Table A.5 C^{eff}_{12} (*GPa*) from the stiffness matrix

v_f	*E4S*	*E6S*	*U4S*	*U6S*	*E4C*	*E6C*	*U4C*	*U6C*
5.23E-07	2.9383	2.9383	4.0617	4.0617	2.9383	2.9383	4.0617	4.0617
5.23E-04	2.9401	2.9401	4.0642	4.0641	2.94	2.94	4.064	4.064
4.19E-03	2.9529	2.9526	4.0816	4.081	2.9519	2.9518	4.0802	4.08
3.35E-02	3.0552	3.0529	4.2206	4.2165	3.0473	3.0464	4.2097	4.208
0.1	3.2873	3.2805	4.5362	4.5237	3.264	3.208	4.503	4.499
0.27	3.8734	3.8554	5.333	5.3	3.81	3.803	5.245	5.232

Table A.6 C^{eff}_{13} (GPa) from the stiffness matrix

v_f	*E4S*	*E6S*	*U4S*	*U6S*	*E4C*	*E6C*	*U4C*	*U6C*
5.23E-07	2.9383	2.9383	4.0617	4.0617	2.9383	2.9383	4.0617	4.0167
5.23E-04	2.9401	2.9401	4.0642	4.0641	2.9402	2.9397	4.0644	4.0636
4.19E-03	2.9526	2.9526	4.0811	4.0811	2.9538	2.9496	4.0828	4.077
3.35E-02	3.0532	3.0528	4.217	4.2162	3.0629	3.0288	4.2304	4.184
0.1	3.2814	3.2801	4.5252	4.523	3.31	3.208	4.565	4.426
0.27	3.8576	3.8543	5.304	5.2998	3.935	3.662	5.411	5.039

Table A.7 S^{eff}_{11} ($10^{-9}\ m^2/N$) from the compliance matrix

v_f	*E4S*	*E6S*	*U4S*	*U6S*
5.23E-07	0.2941	0.2941	0.2128	0.2128
5.23E-04	0.2938	0.2938	0.2126	0.2125
4.19E-03	0.2918	0.2917	0.2111	0.211
3.35E-02	0.2763	0.2757	0.2002	0.1997
0.1	0.2466	0.2453	0.1793	0.178
0.27	0.1941	0.1921	0.1419	0.1399

Table A.8 S^{eff}_{33} ($10^{-9}\ m^2/N$) from the compliance matrix

v_f	*E4S*	*E6S*	*U4S*	*U6S*
5.23E-07	0.2941	0.2941	0.2128	0.2128
5.23E-04	0.2938	0.2938	0.2126	0.2125
4.19E-03	0.2917	0.2917	0.2111	0.211
3.35E-02	0.276	0.2757	0.1999	0.1996
0.1	0.2459	0.2452	0.1786	0.1779
0.27	0.1929	0.1918	0.1407	0.1396

Table A.9 S^{eff}_{44} (10^{-9} m^2/N) from the compliance matrix

v_f	*E4S*	*E6S*	*U4S*	*U6S*
5.23E-07	0.3971	0.3971	0.2872	0.2872
5.23E-04	0.3964	0.3964	0.2868	0.2868
4.19E-03	0.3915	0.3918	0.2836	0.2838
3.35E-02	0.3566	0.3587	0.2602	0.2621
0.1	0.2966	0.301	0.2192	0.2232
0.27	0.2082	0.241	0.1569	0.1624

Table A.10 S^{eff}_{66} (10^{-9} m^2/N) from the compliance matrix

v_f	*E4S*	*E6S*	*U4S*	*U6S*
5.23E-07	0.3971	0.3971	0.2872	0.2872
5.23E-04	0.3964	0.3963	0.2868	0.2867
4.19E-03	0.3919	0.3912	0.2839	0.2833
3.35E-02	0.3595	0.3546	0.2628	0.2584
0.1	0.3027	0.2925	0.2247	0.2154
0.27	0.2163	0.2028	0.1646	0.1516

Table A.11 S^{eff}_{12} (10^{-9} m^2/N) from the compliance matrix

v_f	*E4S*	*E6S*	*U4S*	*U6S*
5.23E-07	-0.1029	-0.1029	-0.0745	-0.0745
5.23E-04	-0.1028	-0.1028	-0.0744	-0.0744
4.19E-03	-0.102	-0.102	-0.0738	-0.0738
3.35E-02	-0.0961	-0.0957	-0.0697	-0.0693
0.1	-0.0848	-0.0839	-0.0618	-0.0608
0.27	-0.0653	-0.0638	-0.0479	-0.0465

Table A.12 S^{eff}_{13} (10^{-9} m^2/N) from the compliance matrix

v_f	*E4S*	*E6S*	*U4S*	*U6S*
5.23E-07	-0.1029	-0.1029	-0.0745	-0.0745
5.23E-04	-0.1028	-0.1028	-0.0744	-0.0744
4.19E-03	-0.102	-0.102	-0.0738	-0.0738
3.35E-02	-0.0958	-0.0957	-0.0694	-0.0693
0.1	-0.0841	-0.0838	-0.0611	-0.0608
0.27	-0.0641	-0.0638	-0.0468	-0.0463

Table A.13 e^{eff}_{13} (C/m^2) from the piezoelectric matrix

v_f	*E4S*	*E6S*	*U4S*	*U6S*	*E4C*	*E6C*	*U4C*	*U6C*
5.23E-07	-1.094E-09	-1.97E-10	-1.081E-09	-1.93E-10	-1.14E-07	-2.20E-08	-1.57E-07	-3.20E-08
5.23E-04	-1.09E-06	-1.97E-07	-1.08E-06	-1.93E-07	-1.00E-04	-2.23E-05	-2.00E-04	-3.07E-05
4.19E-03	-8.75E-06	-1.57E-06	-8.65E-06	-1.55E-06	-9.00E-04	-2.00E-04	-1.30E-03	-2.00E-04
3.35E-02	-7.00E-05	-1.26E-05	-6.92E-05	-1.24E-05	-7.30E-03	-1.40E-03	-1.00E-02	-2.00E-03
0.1	-0.0002	-3.76E-05	-2.00E-04	-3.69E-05	-2.18E-02	-4.30E-03	-3.00E-02	-5.90E-03
0.27	-0.0006	-0.0001	-6.00E-04	-1.00E-04	-5.83E-02	-1.14E-02	-8.03E-02	-1.57E-02

Table A.14 e^{eff}_{33} (C/m^2) from the piezoelectric matrix

v_f	*E4S*	*E6S*	*U4S*	*U6S*	*E4C*	*E6C*	*U4C*	*U6C*
5.23E-07	3.484E-09	2.318E-09	3.45E-09	2.31E-09	8.84E-06	3.95E-06	8.81E-06	3.94E-06
5.23E-04	3.48E-06	2.318E-06	3.45E-06	2.31E-06	8.80E-03	3.90E-03	8.80E-03	3.90E-03
4.19E-03	2.79E-05	1.85E-05	2.76E-05	1.85E-05	7.07E-02	3.16E-02	7.05E-02	3.15E-02
3.35E-02	2.23E-04	1.48E-04	2.21E-04	1.48E-04	5.66E-01	2.53E-01	5.64E-01	2.52E-01
0.1	0.0007	4.43E-04	7.00E-04	4.00E-04	1.69E+00	7.55E-01	1.68E+00	7.54E-01
0.27	0.0018	0.0012	1.80E-03	1.20E-03	4.53E+00	2.02E+00	4.51E+00	2.02E+00

Table A.15 e^{eff}_{15} (C/m^2) from the piezoelectric matrix

v_f	*E4S*	*E6S*	*U4S*	*U6S*	*E4C*	*E6C*	*U4C*	*U6C*
5.23E-07	7.63E-09	7.973E-09	7.19E-09	7.42E-09	1.40E-08	1.50E-08	1.40E-08	1.40E-08
5.23E-04	7.63E-06	7.973E-06	7.19E-06	7.42E-06	1.43E-05	1.49E-05	1.35E-05	1.40E-05
4.19E-03	6.10E-05	6.38E-05	5.75E-05	5.94E-01	1.00E-04	1.00E-03	1.00E-04	1.00E-04
3.35E-02	4.88E-04	5.10E-04	4.60E-04	4.75E-01	9.00E-04	1.00E-03	9.00E-04	9.00E-04
0.1	0.0015	0.0015	1.40E-03	1.40E-03	0.0027	2.80E-03	2.60E-03	2.70E-03
0.27	0.0039	0.004	3.70E-03	3.80E-03	0.0073	7.60E-03	6.90E-03	7.10E-03

Table A.16 K^{eff}_{11} $(10^{-10}\ C/Vm)$ from the permittivity matrix

v_f	*E4S*	*E6S*	*U4S*	*U6S*	*E4C*	*E6C*	*U4C*	*U6C*
5.23E-07	0.452	0.452	0.328	0.328	0.452	0.52	0.328	0.328
5.23E-04	0.4522	0.4522	0.3282	0.3282	0.4525	0.452	0.3283	0.3283
4.19E-03	0.4539	0.4539	0.3294	0.3294	0.4558	0.4557	0.3307	0.3307
3.35E-02	0.4671	0.467	0.3389	0.3389	0.482	0.482	0.35	0.35
0.1	0.497	0.4967	0.3607	0.3605	0.542	0.54	0.393	0.393
0.27	0.5726	0.5718	0.4156	0.4152	0.69	0.689	0.5	0.501

Table A.17 K^{eff}_{33} $(10^{-10}\ C/Vm)$ from the permittivity matrix

v_f	*E4S*	*E6S*	*U4S*	*U6S*	E4C	*E6C*	*U4C*	*U6C*
5.23E-07	0.452	0.452	0.328	0.328	0.452	0.452	0.328	0.328
5.23E-04	0.4522	0.4522	0.3282	0.3282	0.4832	0.4696	0.3592	0.3457
4.19E-03	0.4539	0.4539	0.3294	0.3294	0.7015	0.5927	0.578	0.4693
3.35E-02	0.4671	0.467	0.339	0.3389	2.248	1.578	2.328	1.458
0.1	0.497	0.4967	0.3607	0.3605	6.411	3.814	6.299	3.702
0.27	0.5726	0.5717	0.4156	0.4151	16.42	9.46	16.33	9.369

APPENDIX B

NUMERICAL SOLUTION RESULT

In the following tables, stress and strain fields as well as electric and electric displacement fields at the center of the spherical inhomogeneity for different volume fractions of the piezoceramic have been shown. Again, *E* stands for *Epoxy*, *U* for *UPR*, *4* for *PZT4*, *6* for *PZT6* and the loading conditions are $\sigma^{\circ}_{1} = \sigma^{\circ}_{2} = \sigma^{\circ}_{3} = 25Pa$, $E^{\circ}_{i} = 0$.

Table B.1 Stress field, σ (Pa), for *E4* piezocomposite

v_f	σ_x	σ_y	σ_z	σ_{yz}	σ_{xz}	σ_{xy}
5.23E-07	36	36	35.965	-4.43E-03	-0.1875	-1.41E-02
5.23E-04	35.767	35.824	35.84	-1.53E-03	-2.58E-03	-3.44E-03
4.19E-03	35.625	35.504	35.579	-5.99E-04	3.16E-04	6.76E-04
3.35E-02	34.881	34.884	34.939	-2.97E-01	-3.44E-03	-1.90E-03
0.1	33.715	33.708	33.716	-9.09E-03	-1.06E-02	-9.17E-03
0.27	31.037	31.042	31.146	-2.31E-02	-2.32E-02	-2.27E-02

Table B.2 Stress field, σ (Pa), for *E6* piezocomposite

v_f	σ_x	σ_y	σ_z	σ_{yz}	σ_{xz}	σ_{xy}
5.23E-07	35.979	36.143	35.993	-4.68E-03	-5.07E-03	1.01E-02
5.23E-04	35.694	35.833	35.868	-2.42E-03	-3.93E-03	-3.44E-03
4.19E-03	35.704	35.495	35.601	-1.74E-03	-8.33E-04	-6.44E-04
3.35E-02	34.877	34.883	34.899	-2.28E-03	-2.48E-03	-2.26E-03
0.1	33.599	33.607	33.493	-9.26E-03	-6.23E-03	-0.00684
0.27	30.731	30.753	30.413	-5.12E-02	-5.04E-02	-7.66E-02

Table B.3 Stress field, σ (Pa), for *U4* piezocomposite

v_f	σ_x	σ_y	σ_z	σ_{yz}	σ_{xz}	σ_{xy}
5.23E-07	35.738	35.933	35.709	-4.20E-03	-1.80E-03	-1.30E-02
5.23E-04	35.512	35.565	35.586	-1.30E-03	-2.40E-03	-3.30E-03
4.19E-03	35.372	35.256	35.335	-5.80E-04	3.30E-04	6.50E-04
3.35E-02	34.653	34.656	34.712	-2.80E-03	-3.30E-03	-1.80E-03
0.1	33.52	33.513	33.523	-8.80E-03	-1.00E-02	-8.80E-03
0.27	30.983	31.001	31.1	-7.50E-02	-7.40E-02	-6.80E-02

Table B.4 Stress field, σ (Pa), for *U6* piezocomposite

v_f	σ_x	σ_y	σ_z	σ_{yz}	σ_{xz}	σ_{xy}
5.23E-07	35.734	35.884	35.754	-4.40E-03	-4.80E-03	-9.60E-01
5.23E-04	35.455	35.588	35.631	-2.30E-03	-3.80E-03	3.30E-03
4.19E-03	35.462	35.262	35.373	-1.70E-03	7.70E-04	-6.10E-04
3.35E-02	34.661	34.667	34.689	-2.20E-03	-2.40E-03	-2.20E-03
0.1	33.419	33.427	33.319	-6.00E-03	-6.60E-03	-8.90E-03
0.27	30.622	30.643	30.312	-5.00E-02	-4.90E-02	-7.40E-02

Table B.5 Strain field, ε (10^{-9}), for *E4* piezocomposite

v_f	ε_x	ε_y	ε_z	ε_{yz}	ε_{xz}	ε_{xy}
5.23E-07	1.33E-01	1.36E-01	1.27E-01	-1.15E-04	-5.82E-05	-4.70E-04
5.23E-04	1.32E-01	1.33E-01	1.28E-01	-4.30E-05	-6.45E-05	-1.15E-04
4.19E-03	1.33E-01	1.31E-01	1.27E-01	-9.88E-06	7.50E-06	2.25E-05
3.35E-02	1.29E-01	1.29E-01	1.25E-01	-8.42E-05	-9.18E-05	-6.32E-05
0.1	1.25E-01	1.25E-01	1.20E-01	-2.22E-04	-2.53E-04	-3.06E-04
0.27	1.15E-01	1.15E-01	1.12E-01	-5.71E-04	-5.58E-04	-7.55E-04

Table B.6 Strain field, ε (10^{-9}), for *E6* piezocomposite

v_f	ε_x	ε_y	ε_z	ε_{yz}	ε_{xz}	ε_{xy}
5.23E-07	1.27E-01	1.28E-01	1.19E-01	-1.49E-04	-1.71E-04	-1.88E-04
5.23E-04	1.26E-01	1.27E-01	1.19E-01	-8.06E-05	-1.27E-04	-6.37E-05
4.19E-03	1.27E-01	1.25E-01	1.18E-01	-5.39E-05	-2.16E-05	-1.19E-05
3.35E-02	1.23E-01	1.23E-01	1.16E-01	-7.06E-05	-7.72E-05	-4.19E-05
0.1	1.19E-01	1.19E-01	1.11E-01	-1.89E-04	-2.09E-04	-1.72E-04
0.27	1.09E-01	1.09E-01	9.96E-02	-1.56E-03	-1.53E-03	-1.42E-03

Table B.7 Strain field, ε (10^{-9}), for *U4* piezocomposite

v_f	ε_x	ε_y	ε_z	ε_{yz}	ε_{xz}	ε_{xy}
5.23E-07	1.32E-01	1.35E-01	1.27E-01	-1.08E-04	-5.48E-05	-4.40E-04
5.23E-04	1.31E-01	1.32E-01	1.27E-01	-3.79E-05	-6.05E-05	-1.10E-04
4.19E-03	1.32E-01	1.30E-01	1.26E-01	-9.79E-06	7.76E-06	2.15E-05
3.35E-02	1.28E-01	1.29E-01	1.24E-01	-8.00E-05	-8.71E-05	-6.02E-05
0.1	1.24E-01	1.24E-01	1.20E-01	-2.14E-04	-2.42E-05	-2.93E-04
0.27	1.15E-01	1.15E-01	1.11E-01	-1.92E-03	-1.80E-03	-2.26E-03

Table B.8 Strain field, ε (10^{-9}), for *U6* piezocomposite

v_f	ε_x	ε_y	ε_z	ε_{yz}	ε_{xz}	ε_{xy}
5.23E-07	1.26E-01	1.27E-01	1.18E-01	-1.77E-04	-1.41E-04	-1.61E-04
5.23E-04	1.25E-01	1.26E-01	1.18E-01	-6.17E-05	-7.55E-05	-1.23E-04
4.19E-03	1.26E-01	1.24E-01	1.17E-01	-1.14E-05	-5.16E-04	-1.99E-05
3.35E-02	1.22E-01	1.22E-01	1.15E-01	-4.01E-04	-6.77E-05	-7.39E-05
0.1	1.18E-01	1.13E-01	1.10E-01	-1.66E-04	-1.83E-04	-2.02E-04
0.27	1.09E-01	1.09E-01	9.93E-02	-1.38E-03	-1.53E-03	-1.49E-03

Table B.9 Electric fields, E (V/m) and D (C/m^2), for *E4* piezocomposite

v_f	E_x	E_y	E_z	D_x	D_y	D_z
5.23E-07	3.46E-05	1.39E-04	-0.1192	-3.65E-13	-2.17E-13	-1.59E-02
5.23E-04	8.62E-05	3.89E-05	-0.1228	-6.32E-14	-1.75E-13	-3.13E-13
4.19E-03	-1.15E-05	3.26E-05	-0.1212	-3.24E-15	1.28E-13	4.62E-15
3.35E-02	1.00E-04	7.42E-05	-0.1199	-2.49E-13	-3.56E-13	2.61E-13
0.1	3.80E-04	3.15E-04	-0.1147	5.33E-14	-9.01E-14	-8.84E-13
0.27	8.25E-04	7.84E-04	-0.1083	2.05E-14	-4.08E-13	-1.46E-12

Table B.10 Electric fields, E (V/m) and D (C/m^2), for *E6* piezocomposite

v_f	E_x	E_y	E_z	D_x	D_y	D_z
5.23E-07	9.28E-05	1.40E-04	-0.181	-4.54E-13	-1.80E-13	2.34E-13
5.23E-04	1.04E-04	5.14E-05	-0.1821	-2.09E-13	-1.86E-13	1.28E-13
4.19E-03	5.41E-05	6.10E-01	-0.1798	9.55E-14	-2.81E-14	-5.09E-14
3.35E-02	8.33E-06	8.06E-05	-0.1764	-5.55E-14	-3.55E-14	-1.91E-14
0.1	2.54E-04	2.41E-04	-0.168	-4.93E-14	-3.22E-15	-1.25E-13
0.27	1.93E-03	1.85E-03	-0.1504	-1.15E-13	-6.02E-13	-2.47E-12

Table B.11 Electric fields, E (V/m) and D (C/m^2), for *U4* piezocomposite

v_f	E_x	E_y	E_z	D_x	D_y	D_z
5.23E-07	3.20E-05	1.30E-04	-0.1186	-3.48E-08	-2.07E-13	-1.48E-12
5.23E-04	8.17E-05	3.33E-06	-0.122	-5.31E-14	-1.60E-13	-3.12E-13
4.19E-03	-1.20E-05	3.12E-05	-0.1205	-4.15E-15	1.18E-13	9.12E-15
3.35E-02	9.54E-05	7.11E-05	-0.1192	-2.35E-13	-3.34E-13	2.45E-13
0.1	3.65E-04	3.04E-04	-0.1087	-4.92E-13	-3.07E-12	-6.90E-12
0.27	2.59E-03	2.40E-03	-0.1087	-3.49E-07	-3.07E-12	-6.80E-12

Table B.12 Electric fields, E (V/m) and D (C/m^2), for *U6* piezocomposite

v_f	E_x	E_y	E_z	D_x	D_y	D_z
5.23E-07	8.66E-05	1.33E-04	-0.1799	-4.27E-13	-1.69E-13	2.16E-13
5.23E-04	1.02E-04	4.62E-05	-0.1809	-1.97E-13	-1.81E-13	1.87E-13
4.19E-03	5.00E-05	5.85E-05	-0.1787	9.19E-14	-2.69E+12	-4.90E-14
3.35E-02	7.97E-05	7.72E-05	-0.1754	-5.30E-14	3.33E-14	-1.77E-14
0.1	2.45E-04	2.33E-04	-0.1672	-4.00E-14	-2.43E-15	-1.22E-13
0.27	1.87E-03	1.79E-03	-0.1505	-9.99E-14	-5.74E-13	-2.40E-12

Table B.13 The independent and non-zero components of effective compliance matrix for E4 piezocomposite at different volume fraction of the sphere piezocomceramic

v_f	S^{ef}_{11}	S^{ef}_{33}	S^{ef}_{44}	S^{ef}_{66}	S^{ef}_{12}	S^{ef}_{13}
5.2E-07	0.2941	0.2941	0.54132	0.49904	-0.1029	-0.1029
0.00052	0.2954	0.2954	0.54066	0.49082	-0.1029	-0.1029
0.00419	0.295	0.295	0.55406	0.50106	-0.102	-0.102
0.03349	0.2967	0.294	0.4915	0.4104	-0.1004	-0.1013
0.1	0.2987	0.2935	0.50566	0.4453	-0.097	-0.1012
0.26795	0.2978	0.2962	0.4532	0.4333	0.10118	-0.1011

REFERENCES

1. R. E. Newnham, D. P. Skinner and L. E. Cross, *Connectivity and piezoelectric-pyroelectric composites*, Materials Research Bulletin, Vol. 13, Issue 5, May 1978, pp. 525-536.
2. J.D. Eshelby, *The determination of the elastic field of an ellipsoidal inclusion, and related problems*, Proceedings of the Royal Society of London. Series A, Mathematical and Physical Sciences, Vol. 241, No. 1226, Aug. 20, 1957, pp. 376–396.
3. B. Wang, *Three-dimensional analysis of an ellipsoidal inclusion in a piezoelectric material*, Int. J. Solids Structures, Vol. 29, No.3, 1992, pp. 293-308.
4. H. Fan, S. Qin, *A piezoelectric sensor embedded in a non-piezoelectric matrix*, Int. J. Engineering Science, Vol. 33., No.3, 1995, pp. 379-388.
5. T.L. Jordan, Z. Ounaies, *Piezoelectric Ceramics Characterization*, ICASE NASA Langley Research Center, Hampton, Virginia, 2001.
6. A.J. Moulson, J. M. Herbert, *Electroceramics*, John Wiley and Son Ltd., 2nd Edition, 2003, UK.
7. H. Berger, S. Kari, U. Gabbert, *An Analytical and numerical approach for calculating effective material coefficient of piezoelectric fiber composites*, Int. J. Solids Structures, Article in press.

8. T. Mura, *Micromechanics of defects in solids*, Martinus Nijhoff Publishers, 2nd Edition, 1987, Dordrecht.
9. C. Poizat, M. Sester, *Effective properties of composite with embedded piezoceramic fibers*, Computational Materials Science, Vol. 16, Issue 1-4, pp. 89-97, 1999.
10. C. E. Knight, *The finite element method in mechanical design*, PWS-KENT publishing company, 1993, Boston.
11. *ANSYS 9.0, Theory Reference.*
12. K. Han, Y. Roh, *The performance of a 1-3 mode piezocomposite ultrasonic transducer in relation to the properties of its polymer matrix*, Sensors and Actuators Series A, Physical, Vol. 5, Issue 2, 1999, pp. 176-185.
13. http://www.hepworthcomposites.co.uk/dmc.html

BIOGRAPHICAL INFORNMATION

Solmaz Torabi was born in Tehran, Iran in 1981. She received her B.S. in Materials Science and engineering from the Sharif University of Technology in Tehran, Iran in 2003 and her M.S. in the same major from the University of Texas at Arlington in 2005. She is going to start her Ph.D. in fall 2005. Her research interests include Nanotechnology, MEMS, Electrical Properties of the Materials and FEM analysis of them.